A Section 508–conformant HTML version of this article is available at https://doi.org/10.1289/EHP13913.

Long-Term Exposure to Polystyrene Microspheres and High-Fat Diet–Induced Obesity in Mice: Evaluating a Role for Microbiota Dysbiosis

Zhian Zhai,[1] Ying Yang,[1] Sheng Chen,[2,3] and Zhenlong Wu[1,4]

[1]Department of Companion Animal Science, State Key Laboratory of Animal Nutrition and Feeding, China Agricultural University, Beijing, China
[2]State Key Lab of Chemical Biology and Drug Discovery, Hong Kong Polytechnic University, Kowloon, Hong Kong, China
[3]Department of Food Science and Nutrition, Hong Kong Polytechnic University, Kowloon, Hong Kong, China
[4]Beijing Advanced Innovation Center for Food Nutrition and Human Health, China Agricultural University, Beijing, China

Background: Microplastics (MPs) have become a global environmental problem, emerging as contaminants with potentially alarming consequences. However, long-term exposure to polystyrene microspheres (PS-MS) and its effects on diet-induced obesity are not yet fully understood.

Objectives: We aimed to investigate the effect of PS-MS exposure on high-fat diet (HFD)–induced obesity and underlying mechanisms.

Methods: In the present study, C57BL/6J mice were fed a normal diet (ND) or a HFD in the absence or presence of PS-MS via oral administration for 8 wk. Antibiotic depletion of the microbiota and fecal microbiota transplantation (FMT) were performed to assess the influence of PS-MS on intestinal microbial ecology. We performed 16S rRNA sequencing to dissect microbial discrepancies and investigated the dysbiosis-associated intestinal integrity and inflammation in serum.

Results: Compared with HFD mice, mice fed the HFD with PS-MS exhibited higher body weight, liver weight, metabolic dysfunction-associated steatotic liver disease (MASLD) activity scores, and mass of white adipose tissue, as well as higher blood glucose and serum lipid concentrations. Furthermore, 16S rRNA sequencing of the fecal microbiota revealed that mice fed the HFD with PS-MS had greater α-diversity and greater relative abundances of *Lachnospiraceae*, *Oscillospiraceae*, *Bacteroidaceae*, *Akkermansiaceae*, *Marinifilaceae*, *Deferribacteres*, and *Desulfovibrio*, but lower relative abundances of *Atopobiaceae*, *Bifidobacterium*, and *Parabacteroides*. Mice fed the HFD with PS-MS exhibited lower expression of MUC2 mucin and higher levels of lipopolysaccharide and inflammatory cytokines [tumor necrosis factor-α (TNF-α), interleukin-6 (IL-6), IL-1β, and IL-17A] in serum. Correlation analyses revealed that differences in the microbial flora of mice exposed to PS-MS were associated with obesity. Interestingly, microbiota-depleted mice did not show the same PS-MS–associated differences in Muc2 and Tjp1 expression in the distal colon, expression of inflammatory cytokines in serum, or obesity outcomes between HFD and HFD + PS-MS. Importantly, transplantation of feces from HFD + PS-MS mice to microbiota-depleted HFD-fed mice resulted in a lower expression of mucus proteins, higher expression of inflammatory cytokines, and obesity outcomes, similar to the findings in HFD + PS-MS mice.

Conclusions: Our findings provide a new gut microbiota-driven mechanism for PS-MS–induced obesity in HFD-fed mice, suggesting the need to reevaluate the adverse health effects of MPs commonly found in daily life, particularly in susceptible populations. https://doi.org/10.1289/EHP13913

Introduction

Over the last few decades, the global prevalence of obesity has progressively risen, coinciding with changes in dietary and lifestyle patterns.[1] According to data from the World Health Organization, in 1975, only 2.8% of the global population were considered obese, whereas by 2016, this figure had risen to 13% of adults, or ∼650 million people globally.[2] Obesity negatively affects physiological functions and poses a significant threat to public health. It heightens the risk of developing metabolic syndromes such as type 2 diabetes, cardiovascular disease,[3] and metabolic dysfunction-associated steatotic liver disease (MASLD; formally known as nonalcoholic fatty liver disease).[4] Obesity is influenced by a combination of genetic, epigenetics, and environmental factors, including lifestyle and eating habits.[5] Excessive energy intake, often resulting from the consumption of energy-rich diet such as a high-fat diet (HFD), is associated with obesity,[6] and increasing evidence has shown that long-term consumption of a HFD changes the composition of the intestinal microbiota and leads to dysbiosis in mice.[7] The intestinal microbiota plays a crucial role in regulating several aspects vital to host metabolic function, such as fat accumulation, hepatic lipogenesis, and energy absorption.[8,9] Despite dietary factors, other environmental factors, such as polysorbate-80 and carboxymethylcellulose, two commonly used food additives, have also been proven to promote obesity through intestinal microbiota alteration.[10] Therefore, comprehending the correlation between diet and other environmental factors is imperative in developing comprehensive approaches to mitigate obesity.

Microplastics (MPs), a class of emerging persistent environmental pollutants, are composed of chemically fragmented plastic particles, fibers, and fragments <5 mm in diameter.[11] If current production and waste management trends persist, ∼12,000 million metric tons of plastic waste will accumulate in landfills or the natural environment by 2050,[12] and then time results in gradual physicochemical degradation of plastics into smaller-size particles (secondary MPs).[13] Moreover, primary microplastics can also be present in the form of microbeads. Initially, these tiny beads were commonly discovered in health and beauty products, such as face washes and toothpastes.[14] Microplastics are ubiquitous in the environment and pose a potential threat to the ecosystem and human health.[14,15] Humans may be subjected to exposure to MPs through inhalation and ingestion.[16] Daily intakes of MPs ranging between 0.5 and 10 μm for adults from mineral water in plastic bottles have been estimated at 40.1 μg/kg body weight (BW) per day.[17] Shockingly, MPs have been found in urine,[18] fecal,[19] blood,[20] colectomy specimens,[21] placenta, and meconium of human.[22] As a result, serious concerns regarding their potential toxicity to humans have been raised, and their general toxicological effects on organisms need to be further

Address correspondence to Zhenlong Wu, Department of Companion Animal Science, China Agricultural University, Beijing 100193, China. Telephone: 86-10-6273-1003. Email: wuzhenlong@cau.edu.cn

Supplemental Material is available online (https://doi.org/10.1289/EHP13913).

The authors affirm that they have no known financial interests or personal relationships that could have potentially influenced or biased the findings presented in this research paper.

Conclusions and opinions are those of the individual authors and do not necessarily reflect the policies or views of EHP Publishing or the National Institute of Environmental Health Sciences.

Received 31 August 2023; Revised 23 July 2024; Accepted 8 August 2024; Published 3 September 2024.

evaluated. Polystyrene (PS) is a commonly used polymer in the production of Styrofoam, which is widely used in food containers and packaging.[23,24] Research has shown that PS microspheres (PS-MS) with a diameter of 5 μm can accumulate in the intestine, resulting in dysfunction of the intestinal barrier and alteration of metabolites in the serum in otherwise healthy mice.[25–27] Furthermore, PS-MS of a diameter within 0.5–5 μm have been extensively employed in bioassays to investigate biological interactions and toxicity in living organisms.[28–30] It should also be noted that prolonged exposure to high doses of polyethylene MS in mice can lead to apparent adverse effects, such as histological injury and inflammation of the colon.[31]

Besides these advances, the potential impacts of PS-MS on gut microbiota have been a focus of toxicity studies, given that 99.54% of PS-MS were found to be excreted in feces after oral administration of 5-μm PS-MS in mice.[32] Exposure to PS-MS have been reported to induce anxiety-like behavior in mice by modulating gut microbe homeostasis.[33] Recent study has also associated dysregulation of the gut microbiota with hepatic injuries induced by PS-MS in mice.[34] According to a study, alterations in the composition of gut microbiota were associated with the development of obesity and its associated metabolic disorders.[35] In addition, other studies have demonstrated that gut dysbiosis, which can result from environmental or genetic factors, can impede intestinal integrity in obese animals.[36] Furthermore, the toxic effects of PS-MS are related to dietary changes and disease status in animal models,[37,38] indicating that the toxicity of PS-MS may be amplified in obese populations. Nonetheless, it is still not clear whether PS-MS could disrupt gut barrier function by inducing gut dysbiosis and how PS-MS disrupts the gut microbiota and contributes to HFD-induced obesity. Therefore, it is highly plausible that exposure to PS-MS will induce stress on gut microbiota species, thereby compromising gut integrity and promoting obesity induced by a HFD.

In this study, we investigated the effect of PS-MS via drinking water in a HFD-induced–obesity mouse model for 8 wk. The study also explored the impact of PS-MS on intestinal microbes and colonic mucin levels. Furthermore, downstream inflammation and obesity were assessed to identify potential mechanisms related to PS-MS promoting HFD-induced obesity by focusing on gut microbiota. Antibiotic depletion of the microbiota and fecal microbiota transplantation (FMT) were performed to assess the influence of PS-MS on intestinal microbial ecology.

Materials and Methods

Characterization of PS-MS

An aqueous suspension containing PS-MS at a concentration of 25 mg/mL was procured from Shanghai Macklin Biochemical Technology Co., Ltd. The suspension consisted of beads with a particle size of 5 μm (ranging from 4.0 to 4.9 μm, identified as L815942) and were dispersed in deionized water at a concentration of 5.0% wt/vol. The morphology analysis was conducted using transmission electron microscope spectroscopy (Hitachi, HT7800) (Figure S1). Briefly, The microplastics were suspended in anhydrous ethanol and then dropped onto a support membrane using a dropper while the membrane-covered copper mesh was held in place with forceps. The sample was kept in position until the droplets on the support membrane were completely dried. Subsequently, electron microscopy was used for observation. To ensure optimal dispersion, all suspensions underwent thorough sonication, followed by dilution with water prior to their use.

Animals and Diets

Seventy-two male C57BL/6J mice (24 mice per experiment), aged 6–8 wk, were procured from Vital River Company (Vital River Laboratory Animal Center) and were selected for the experiment. The mice were accommodated in environmentally controlled cages, ensuring a constant temperature of $24 \pm 1^{\circ}C$, relative humidity of $55\% \pm 5\%$, and a standard 12-h light:dark cycle. Groups of mice were housed together ($n = 6$ per group, 3/cage) and provided free access to feed and drinking water. The experimental procedures received approval from the Laboratory Animal Welfare and Animal Experimental Ethical Committee at China Agricultural University (approval No. AW72403202-1-31). To establish a consistent baseline for the intestinal microbiota, all groups of mice were co-housed for a period of 1 wk prior to the commencement of the experiment. The mice were then given either a normal diet (ND; D12450B, 3.85 kcal/g; Research Diet, Inc.) containing 10% kcal from fat or a HFD (D12492, 5.24 kcal/g; Research Diet, Inc.) consisting of 60% kcal from fat. Diet compositions are reported in Table S2. Energy intake (in kilocalories per kilogram BW per day) was calculated as follows: food intake (g/kg BW per day) × food energy content (kcal/g). Suspensions containing 10-mg/L PS-MS were prepared using ultrapure sterile water, followed by sonication for 10 min. Bottles were shaken to ensure an even distribution of the microspheres in the drinking water to prevent sedimentation of the PS.

The mice were assigned to different treatment groups: ND and HFD groups received filtered and autoclaved water, whereas the ND + PS-MS and HFD + PS-MS groups received water supplemented with PS-MS at a dose of 10 mg/L per day. PS-MS water was replaced every 2 d. This treatment regimen was followed for a duration of 8 wk. The water intake was measured every 2 d during treatment and calculated as an average water intake per mouse per day. At the end of the experiment, the mice underwent an overnight fasting period before cervical dislocation euthanasia. Blood samples were collected by eyeball blood sampling and centrifuged at 3,000 rpm for 15 min at 4°C to obtain plasma. The plasma was then preserved at −80°C to facilitate subsequent analysis of blood biochemical indicators. Liver, distal colon, inguinal adipose tissue, epididymal white adipose tissues, and perirenal white adipose tissues were carefully excised and weighed. Two sections were excised from each tissue sample: One was fixed in paraformaldehyde, and the other was stabilized with optimum cutting temperature (O.C.T.) embedding medium. The remaining tissue was swiftly cryopreserved in liquid nitrogen and stored at −80°C.

Histology

The fixed liver, distal colon and inguinal adipose tissues were immersed in a 4% paraformaldehyde solution at room temperature for 24 h, followed by embedding in paraffin for further processing. Hematoxylin and eosin (H&E) staining was conducted on liver distal colon and inguinal adipose tissues sections, which had a thickness of 5 μm, to enable general observations of their morphology. MASLD activity scores (steatosis, inflammation, and ballooning degeneration) were determined according to the procedure described by Kleiner et al.[39] Specifically, steatosis was determined by measuring the percentage of hepatocytes containing lipid droplets, defined as 0 (<5%), 1 (5%–33%), 2 (>33%–66%), or 3 (>66%). Hepatocyte encapsulation was classified into grade 0 (none), grade 1 (very few), and grade 2 (multiple cells/obvious spheroidization). Lobular inflammation score was defined as 0 (no foci), 1 (<2 foci per ×200 field), 2 (2–4 foci per ×200 field), or 3 (>4 foci per ×200 field). To evaluate hepatic lipid accumulation, Oil Red O staining was performed on 8-μm frozen liver sections (livers from 4–5 mice per group were used for staining). The quantification of goblet cells was performed using the Alcian blue/periodic acid-Schiff (AB/PAS) staining technique. All the images were captured using a light microscope (BX63, OLYMPUS), whereas Image-Pro Plus software from Media Cybernetics was used for quantification purposes.

Immunofluorescence Staining

Immunofluorescence staining (IF) was performed on 5-μm frozen sections of the distal colon. The frozen sections were fixed with 4% paraformaldehyde in phosphate-buffered saline (PBS) for 10 min at 4°C. After fixing, the sections were incubated with 5% goat serum in PBS at room temperature for 30 min. Subsequently, primary antibodies against tight junction proteins [Zona occludin-1 (ZO-1)/Tight junction protein-1 (Tjp1), 1:200, # D264329; and Occludin, 1:200, # 13409-1-AP, purchased from Sangon Biotech Co., Ltd. and Proteintech Co., Ltd.] were applied without fluorescent labeling at 4°C overnight. Following that, the sections were incubated with a secondary antibody (Cy3-labeled goat anti-rabbit IgG (H + L), 1:200 # A0516, Biyuntian) labeled with fluorescence for 2 h at room temperature. Nuclei were stained with Hoechst (33342, Thermo Fisher Scientific; 1:1,000) for 1 min, and excess staining solution was removed by rinsing with PBS. Finally, the slides were mounted using an antifluorescence decay mounting medium (# S2100, Beijing Solarbio Science & Technology Co., Ltd.) and observed under laser scanning confocal microscopy (ECLIPSE Ti2, Nikon). Image acquisition was performed using the Nikon NIS-Elements AR imaging software analysis platform. Fluorescence intensity statistics were analyzed using ImageJ.[40]

Quantitative Real-Time Polymerase Chain Reaction

The collected colon tissue samples were ground in liquid nitrogen and stored at –80 °C for further use. Total RNA was extracted from the colon following the manufacturer's instructions of M5 Hiper Total RNA Extraction Reagent (MF034-01, mei5bio) The concentration of total RNA was determined using a Nano Photomeyer P-Class (Implen GmbH). RNA (4,000 ng) was reverse-transcribed into 10 μL of complementary DNA using a reverse transcription kit (Yeasen Biotechnology Co., Ltd., # 11120ES60). The primers used in this experiment are commonly used primers in our laboratory. Subsequently, real-time quantitative PCR (RT-qPCR) was conducted using the SYBR Premix Ex Taq II (Beijing Aidlab Biotechnologies Co., Ltd.) alongside the ABI-Prism 7500 Sequence Detection System (Applied Biosystems). The following program was used for RT-qPCR: 95°C for 3 min, 40 cycles of 95°C for 15 s, and then 60°C for 60 s. The alteration in mRNA expression level was calculated using the $2^{-\Delta\Delta CT}$ method. To standardize the gene expression level, Glyceraldehyde-3-phosphate dehydrogenase (GAPDH) was used. The primers used in this study were designed and saved by our laboratory (Table S1).

Enzyme-Linked Immunosorbent Assay

For this research, ground colon tissue was weighed and homogenized in PBS at 4°C. Homogenates were centrifuged at $14{,}000 \times g$ for 10 min at 4°C. Supernatants were transferred to clean microcentrifuge tubes for detection. The MUC2 level in the collected supernatant was quantified by using a MUC2 enzyme-linked immunosorbent assay (ELISA) kit (# MM-44508M1) in accordance with the prescribed instructions. In addition, serum lipopolysaccharides (LPS; # MM-0634M2) and serum inflammatory factors, including interleukin-1β (IL-1β, # MM-0040M1), IL-6 (# MM-0163M1), tumor necrosis factor-α (TNF-α, # MM-0132M1), and IL-17A (# MM-0170M1), were measured using ELISA kits following the recommended instructions, and the concentration of each cytokine was quantified using a standard curve according to the manufacturer's instructions. All ELISA kits used were procured from Jiangsu Meimian Industrial Corporation.

Oral Glucose Tolerance Test

At week 8, the oral glucose tolerance test was carried out to evaluate the mice's ability to tolerate glucose according to the methods described by a previous study.[41] Mice were deprived of food for 6 h, blood samples were collected from the caudal vein at baseline (0 min) and at various time points (15, 30, 60, 90, and 120 min) after administering 2 g/kg BW glucose through oral gavage, and the area under the curve (AUC) of blood glucose vs. time was calculated. The glucose levels were measured using a glucose analyzer (OneTouch Ultra Easy).

Determination of Plasma Parameters

Plasma biomarkers were quantified using testing kits provided by Nanjing Jiancheng Bioengineering Institute. These biomarkers included total cholesterol (TC; A111-1-1), low-density lipoprotein cholesterol (LDL-C; A113-1-1), high-density lipoprotein cholesterol (HDL-C; A112-1-1), and total triglycerides (TG; A110-1-1).

16S rRNA Sequencing

Every 4 wk, feces were collected from each individual mouse by stroking the back of the mouse to induce defecation and immediately frozen at −80°C until further processing. The Omega Bio-tek Stool DNA Kit was employed to extract microbial DNA from the feces as per the manufacturer's instructions. Bacterial DNA concentrations were determined by employing a NanoDrop 2000 spectrophotometer (Thermo Scientific). The V3–V4 hypervariable region of the bacterial 16S rRNA gene was amplified using universal primers 338F (5′-ACTCCTACGGGAGGCAGCAG-3′) and 806R (5′-GGACTACNNGGGTATCTAAT-3′), with 8-digit barcode sequences added to the 5′ end of each primer for sample identification (provided by Allwegene Company). PCR products were purified using a Beckman Coulter Agencourt AMPure XP Kit. Sequencing libraries were generated using the NEB Next Ultra II DNA Library Prep Kit (New England Biolabs) according to the manufacturer's recommendations. Library quality was assessed by NanoDrop 2000 (Thermo Fisher Scientific), Agilent Bioanalyzer, and ABI StepOnePlus Real-Time PCR System (Applied Biosystems). Deep sequencing was performed on an Illumina MiSeq PE300 platform at Beijing Allwegene Technology Co., Ltd., Beijing, China. After sequencing, image analysis, base calling, and error estimation were performed using Illumina Analysis Pipeline (version 2.6). Raw data were filtered and spliced using Pear software (version 0.9.6; Anaconda), and chimeras were removed using Vsearch software (version 2.7.1). Qualified sequences were clustered into operational taxonomic units (OTUs) using the Uparse algorithm of Vsearch (version 2.7.1) software with a similarity threshold of 97%. OTU unique representative sequences were obtained, and all tags were mapped to each OTU representative sequence using the BLAST tool (http://www.ncbi.nlm.nih.gov/BLAST/). Rarefaction curves were generated, and richness and α-diversity indices (Shannon's index, Simpson's index, and Chao1) were calculated using QIIME (version 1.8.0)[42] based on the OTU abundance information. To assess the dissimilarity between multiple samples, principal component analysis (PCA) was performed using R (version 3.6.0; R Development Core Team) based on the OTU information from each sample. The relative abundances of taxa at multiple levels, including phylum, class, order, family, genus, and species, were computed based on the results of taxonomic annotation and relative abundance. To provide a comprehensive analysis of the microbial diversity differences between samples, Metastats and linear discriminant analysis effect size (LEfSe), were conducted.

Antibiotic Treatment

Antibiotic treatment was administered following an established protocol.[43] In brief, the mice were treated daily via oral intragastric gavage with a broad-spectrum antibiotic cocktail (ABX) (Beijing Suo Lai Bao Technology Co., Ltd.) consisting of ampicillin

(100 mg/kg BW), neomycin (100 mg/kg BW), metronidazole (100 mg/kg BW), and vancomycin (50 mg/kg BW) throughout the 8-wk ND/HFD-feeding period ($n = 6$ per group).

FMT

Recipient mice were administered a mixture of antibiotics [vancomycin (0.5 g/L), neomycin sulfate (1 g/L), metronidazole (1 g/L), and ampicillin (1 g/L); Beijing Suo Lai Bao Technology Co., Ltd] in their drinking water for 7 consecutive d prior to FMT. Fecal transplant was conducted according to established protocols.[44–46] Briefly, 8-wk-old male donor mice were fed either the HFD or the HFD + PS-MS (10 mg/L in drinking water) ($n = 6$ per group), whereas recipient mice were fed microbiota derived from mice fed either the HFD or the HFD + PS-MS ($n = 6$ per group). Fecal samples were collected from the donors by stroking the back of the mouse and pooled over the course of the 8-wk experiment. Donor feces were diluted with PBS (1 g of sample in 10 mL of PBS) and homogenized for 1 min using a vortex to create a liquid slurry. The mixture was centrifuged at $900 \times g$ for 3 min to remove particulate matter. About 200 µL of the supernatant was immediately administered to each recipient mouse by oral gavage three times a week for 8 wk. To prevent alterations in the bacterial makeup, fresh transplant material was readied within a timeframe of 10 min prior to oral gavage.

Statistical Analysis

Analysis of the data was performed using GraphPad software (version 9.0). Unless otherwise indicated, the parametrically distributed data underwent Student's *t*-test for comparisons between two groups, whereas nonparametrically distributed data were analyzed using the Mann–Whitney test, and differences in mean values among more than two groups were determined using one-way analysis of variance (ANOVA) with a Tukey multiple comparison test. The Brown–Forsythe and Welch ANOVA test was performed when the variances were not equal. Multiple unpaired *t*-tests and two-way repeated measures ANOVA with a Tukey multiple comparison test were performed as indicated in figure legends. Correlation statistical analyses are performed by Pearson's correlation by using R (version 3.5.3; R Development Core Team). Statistical significance was considered when $p < 0.05$.

Results

Measures Related to Obesity and Metabolism in Mice Exposed to ND or HFD with and without PS-MS in Drinking Water for 8 Wk

After 8-wk ingestion of PS-MS at a dose of 10 mg/L via drinking water (Figure 1A), mice treated with PS-MS gained a similar amount of weight under ND. However, compared with the HFD group, the HFD + PS-MS group gained >17% more BW (BW relative to week 0: 158.17% ± 8.25 vs. 175.21% ± 5.35; Figure 1B,C), despite consuming less high-fat feed and calories. (Figure 1D). There was no significant difference in daily water consumption in mice exposed to ND or HFD with and without PS (Figure S2). In addition, mice in the PS-MS + ND group showed no significant difference in liver weight compared with the ND group, whereas the PS-MS + HFD group exhibited a greater liver weight compared with the HFD alone group (Figure 1E). Further analysis of liver tissue using H&E and Oil Red O staining revealed that the PS-MS + HFD group exhibited a higher MASLD histological activity score and a larger liver lipid area compared with the HFD group (Figure 1F–I). Although there was no significant difference in adipose tissue weight between the PS-MS group and the PS-MS + ND group, the HFD + PS-MS group did exhibit 76% greater inguinal white adipose tissue (iWAT) mass, 64% greater perirenal white adipose tissue (pWAT) mass, and 39% greater epididymal white adipose tissue (eWAT) mass compared with the HFD alone group (Figure 1J–L). In the H&E analysis of iWAT, no significant differences were observed between the ND and PS-MS + ND groups. However, the HFD + PS-MS group exhibited larger adipocyte sizes compared with the HFD group (Figure 1M,N). The increased obesity may further disrupt insulin signaling, reduce insulin sensitivity, and disturb the stability of blood glucose. Hence, glucose tolerance experiments were conducted in mice. According to Figure 1O, fasting blood glucose concentrations and total glucose AUC in the HFD + PS-MS group were significantly higher compared with HFD-fed mice who received a glucose gavage. In addition, there was no significant difference in fasting blood glucose levels and blood glucose AUC between the ND group and the ND + PS-MS group. Lipid profiles were analyzed biochemically and showed significantly higher levels of TC and TG in the liver (Figure 1P,Q), as well as significantly higher levels of TC, LDL-C, and LDL-C/HDL-C in serum (Figure 1S,T,V) of HFD + PS-MS mice compared with the HFD alone group. There was no difference observed in TG and HDL-C with PS-MS supplementation when compared with the HFD group (Figure 1R,U).

Composition of Gut Microbes in Fecal Samples from Mice Exposed to ND or HFD with and without PS-MS in Drinking Water for 8 Wk

We examined the effects of PS-MS on the composition of gut microbiota by analyzing bacterial 16S rRNA (V3–V4 region) present in feces using MiSeq sequencing-based analysis. Bacterial diversity analysis revealed that the α-diversity indices (Chao1 and Observed species) of gut flora in both HFD- and ND-fed mice were greater in those mice exposed to PS-MS (Figure 2A; Figure S3A). However, the Shannon's diversity index indicated no significant difference among the ND, ND + PS-MS, and HFD groups (Figure S3B). In addition, microbiota composition in both ND and HFD mice were considerably different in mice exposed to PS-MS compared with those not (Figure 2B,C). The Firmicutes-to-Bacteroidetes (F:B) ratio was less than one-half that of the HFD + PS-MS group compared with the HFD group (Figure 2D). At the family levels, abundances of *Lachnospiraceae*, *Oscillospiraceae*, *Marinifilaceae*, *Akkermansiaceae*, and *Deferribacterales* were different in the HFD + PS-MS group compared with HFD group (Figure 2E–G,I,J), and the HFD + PS-MS group had a lower relative abundance of *Bifidobacteriaceae* and *Atopobiaceae* (Figure 2H,K). Family *Deferribacteres* were significantly enriched at higher taxonomic levels such as phylum, class, and order in HFD + PS-MS group compared with the HFD group. At the genus level, compared with the HFD group, the PS-MS + HFD group exhibited a higher relative abundance of *Desulfovibrio*, whereas the relative abundance of *Bifidobacterium* and *Parabacteroides* was lower (Figure 2L–N).

Measures of Intestinal Integrity, Inflammation, and Correlation between Gut Microbiota and Parameters Related to Obesity in Mice Exposed to ND or HFD with and without PS-MS in Drinking Water for 8 Wk

Intestinal dysbiosis may undermine the integrity of the intestinal barrier, facilitating the direct translocation of LPS into the circulatory system, thereby instigating a low-grade inflammatory response.[47] To determine whether PS-MS disrupted gut integrity, we hypothesized that the observed outcomes might be attributed to the impairment of the intestinal barrier. To validate this assumption, we conducted AB-PAS staining. The results revealed notably fewer intestinal goblet cell contents and lower mucin secretion levels in the mice exposed to PS-MS compared with vehicle-exposed

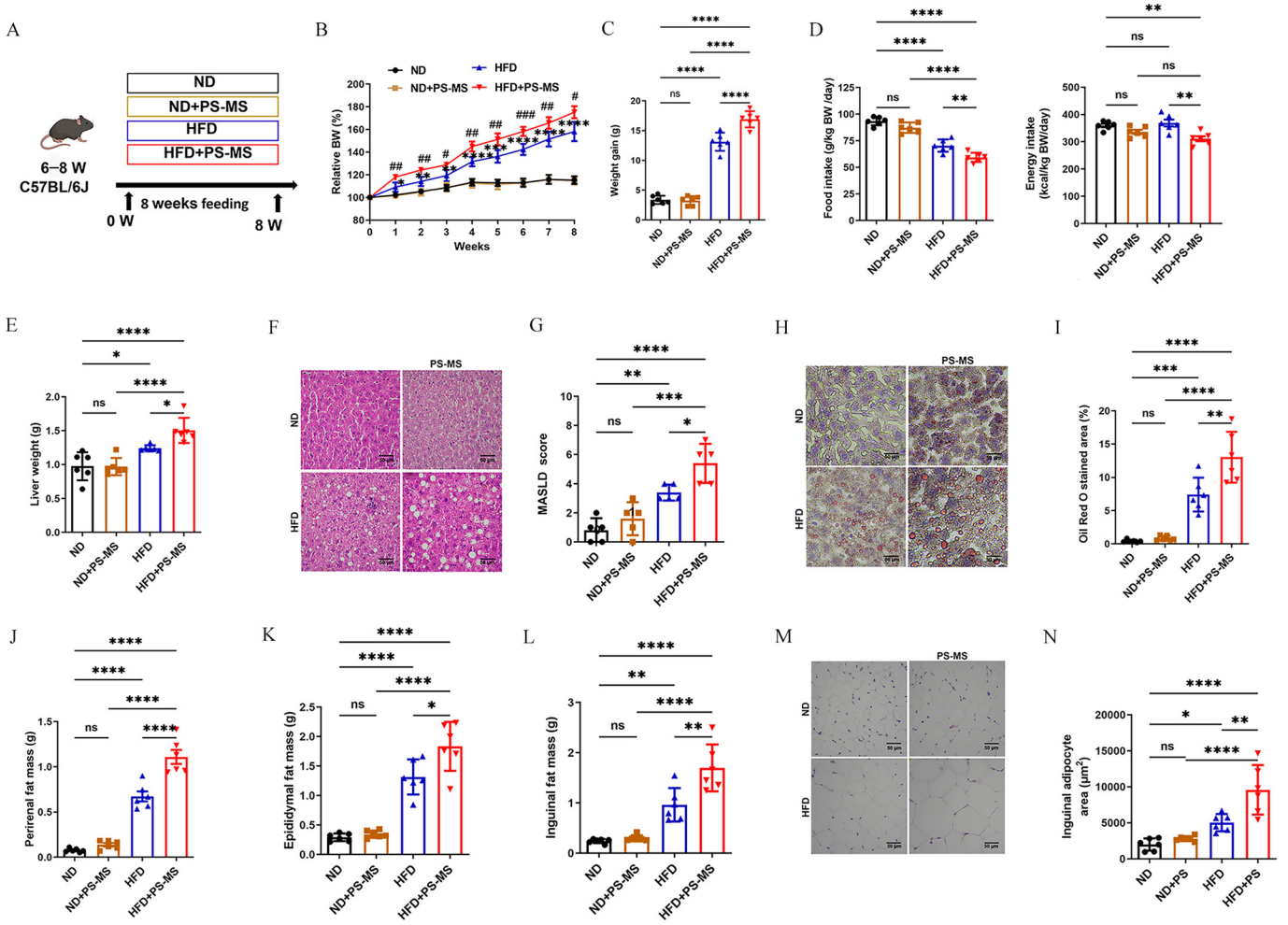

Figure 1. Measures associated with obesity and metabolism measured in mice exposed to ND or HFD with and without PS-MS in drinking water for 8 wk. The ND- and HFD-fed mice were exposed to 10-mg/L PS-MS. (A) Exposure to ND or HFD ± PS-MS started at 8 wk of age. (B) Relative BW calculated as follows: BW(week 8)/BW (week 0); Data were compared using two-way repeated measures ANOVA with a Tukey multiple comparison test for individual time points. (C) BW gain calculated as follows: BW (week 8) – BW (week 0). (D) Food intake and energy intake. (E) Liver weight. (F) Representative microscopic observation of liver tissue by H&E staining. (G) MASLD histological activity score ($n = 5$); each dot on the graph represents one mouse. (H) Oil Red O staining images showing the lipid deposition in liver tissue. (I) Liver lipid deposition area analyzed from Oil Red O staining images; each dot on the graph represents one mouse. Mass of (J) perirenal adipose tissue, (K) epididymal adipose tissue, and (L) inguinal adipose tissue. (M) Representative microscopic observation of adipocyte size of inguinal adipose tissue. (N) Quantification of mean inguinal adipose tissue area; each dot shown on the graph corresponds to one mouse. (O) Fasting blood glucose level and area under the curve (AUC) of blood glucose levels. The liver (P) TC and (Q) TG, as well as serum (R) TG, (S) TC, (T) LDL-C, (U) HDL-C levels and (V) fold changes of LDL-C/HDL-C were measured with the corresponding assay kits. All values are represented as mean ± SD in scatter plots ($n = 6$). Each dot represents one mouse. Data were analyzed using one-way ANOVA with a Tukey multiple comparison test. Corresponding numeric data can be found in Table S3. Note: ANOVA, analysis of variance; BW, body weight; H&E, hematoxylin and eosin; HDL-C, high-density lipoprotein cholesterol; HFD, high-fat diet; LDL-C, low-density lipoprotein cholesterol; MASLD, metabolic dysfunction-associated steatotic liver disease; ND, normal diet; ns, nonsignificant; PS-MS, polystyrene microspheres; SD, standard deviation; TC, total cholesterol; TG, total triglycerides. For (B), $^{\#\#\#}p < 0.001$, $^{\#\#\#\#}p < 0.001$, HFD + PS-MS vs. HFD; $^{**}p < 0.01$; $^{***}p < 0.001$; $^{****}p < 0.0001$, HFD vs. ND. For (C–E,G,I–V), $^{*}p < 0.05$, $^{**}p < 0.01$, $^{***}p < 0.001$, $^{****}p < 0.0001$.

mice, regardless of whether they were fed a ND or a HFD (Figure 3A). The epithelial mucin-encoding gene *Muc2* was less expressed in mice exposed to PS-MS in both the ND and HFD groups (Figure 3B). Similarly, the MUC2 protein levels (ELISA analysis) were also lower in mice exposed to PS-MS (Figure 3C). To assess the integrity of the intestinal barrier in colon tissues, the expression levels of the tight junction proteins, TJP1 and occludin, were determined. The results showed that the mRNA expression levels of *Tjp1* were significantly lower in PS-MS–exposed mice compared with those of control mice (in both ND and HFD groups) (Figure 3D). Meanwhile, expression of Tjp1 and occludin proteins were significantly lower in the distal colon of PS-MS–exposed mice compared with controls (Figure 3E–G). In this study, we investigated the effects of PS-MS on gut microbiota and its potential role in promoting obesity and inflammation. 16S rRNA sequencing results showed greater relative abundance of *Desulfovibrio* genus in PS-MS–exposed mice compared with the control animals in the HFD, but not the ND groups (Figure 2L). Considering the findings mentioned above, we hypothesized that the effects of PS-MS on MUC2, Tjp1, and occludin expression and the measured differences in microbiota following PS-MS exposure could be associated with gut barrier function and thus with inflammation. To further explore this hypothesis, we tested the levels of LPS and downstream inflammatory factors in the serum. The results showed that serum levels of LPS, IL-1β, IL-6, TNF-α, and IL-17A were significantly higher in the HFD + PS-MS group than in the ND group (Figure 3H–L).

To comprehensively analyze the relationship between obesity and gut microbiota, we generated a correlation matrix by calculating Pearson's correlation coefficient. Our heatmap correlation analysis

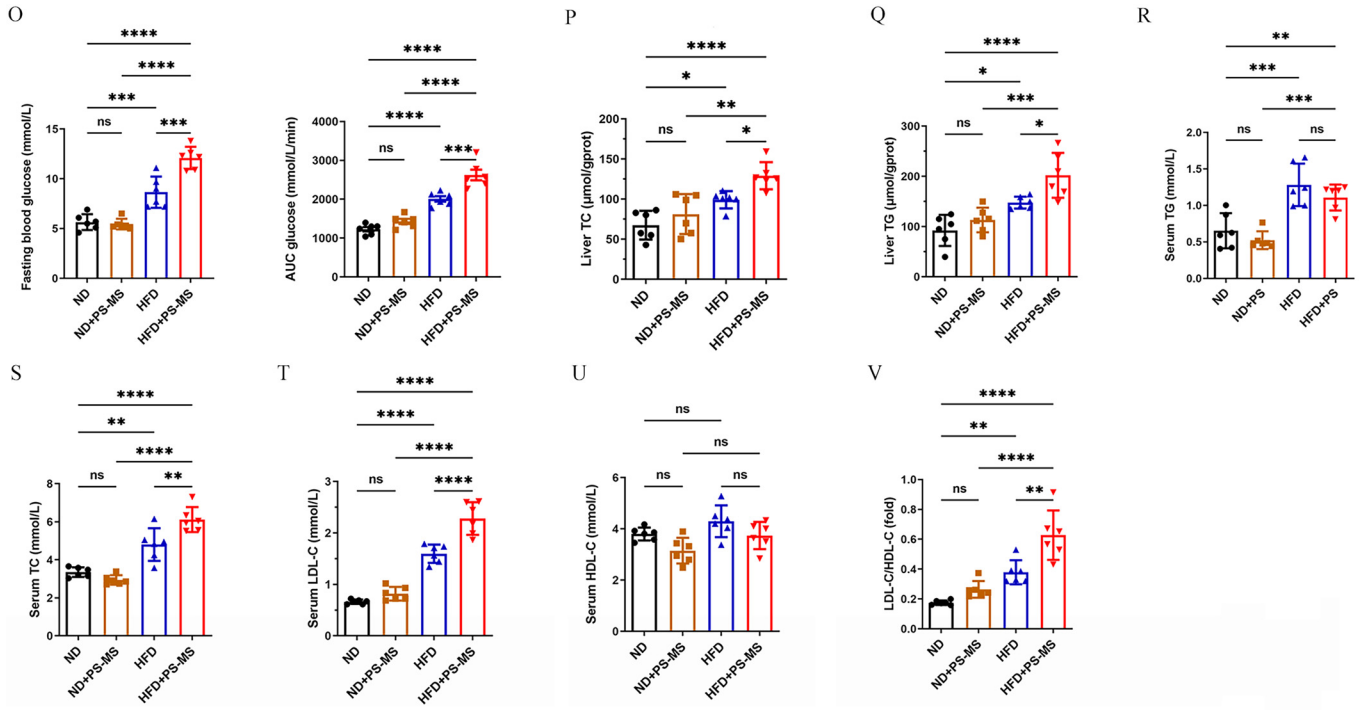

Figure 1. (*Continued.*)

showed that the top 15 families affected by PS-MS intervention were significantly associated with at least one parameter of obesity (Figure 3M). Specifically, *f__Streptococcaceae*, *f__Lachnospiraceae*, *f__Oscillospiraceae*, *f__Desulfovibrionaceae*, and *f__Marinifilaceae* showed significant positive associations with BW gain, epididymal fat, perirenal fat, inguinal adipose accumulation, serum TC, fasting glucose levels, serum TC, liver TC, and liver TG. Conversely, *f__Bifidobacteriaceae* and *f__Atopobiaceae* were positively correlated with colon MUC2 protein levels. Notably, *f__Bacteroidaceae* showed significant positive correlations with serum IL-1β and IL-6 levels. Furthermore, *f__Marinifilaceae* were significantly positively correlated with serum TNF-α and IL-17A levels. In contrast, *f__Prevotellaceae*, *f__Muribaculaceae*, *f__Erysipelotrichaceae*, *f__Bifidobacteriaceae*, and *f__Atopobiaceae* were negatively correlated with weight gain, liver weight, inguinal adipose, perirenal adipose, epididymal adipose, LDL-C, LDL-C/HDL-C, fasting glucose and liver TG, IL-1β, TNF-α, and IL-17A levels. In addition, *f__Lactobacillaceae* were negatively correlated with serum IL-6 levels, whereas *f__Lachnospiraceae*, *f__Oscillospiraceae*, *f__Desulfovibrionaceae*, *f__Marinifilaceae* were negatively associated with MUC2 protein levels. Last, *f__Akkermansiaceae* showed significant negative associations with BW gain, liver weight, epididymal adipose, fasting glucose, and serum TC.

Effects of Antibiotic-Induced Deletion of Gut Flora on Measures Associated with Obesity and Outcomes Related to Metabolism in Mice Exposed to ND or HFD with and without PS-MS in Drinking Water for 8 Wk

The gut microbiota's involvement in diet-induced obesity and metabolic syndrome was suggested by the reduced susceptibility observed in germ-free or microbiota-depleted mice.[48] To further elucidate the role of gut microbiota in diet-induced obesity driven by PS-MS, we employed an ABX-treated mouse model (the broad-spectrum ABX consisting of ampicillin, neomycin, metronidazole, and vancomycin)[43] to investigate the effects of PS-MS on mice fed a ND or a HFD. Following an 8-wk administration of ABX via gavage (Figure 4A), >97% of the intestinal bacteria were eradicated (Figure S4). Notably, the PS-induced obesity outcomes were not detected in mice fed with either the ND or the HFD after receiving ABX treatment. The administration of ABX was found to effectively mitigate the weight gain observed in PS-MS–exposed mice fed a HFD compared with nonexposed HFD-fed mice (Figure 4B,C). However, ABX treatment was not completely resistant to HFD-induced weight gain compared with the ND group (Figure 4B,C). The daily food intake and energy intake in mice in the HFD + PS-MS group were significantly higher compared with the HFD groups, whereas food intake and energy intake were almost similar in the ND groups (Figure 4D). Furthermore, There were no significant differences in fat content in the liver, perirenal adipose tissue, inguinal adipose tissue, and epididymal adipose tissue of mice in the HFD + PS-MS group compared with mice fed a HFD alone (Figure 4E–L). In addition, in mice treated with ABX, there was no significant difference in fasting blood glucose levels between the ND group and the ND + PS-MS group; the blood glucose AUCs in the ND + PS-MS and HFD + PS-MS groups were significantly lower than in the ND and HFD groups, respectively (Figure 4M); and serum lipid levels were similar in HFD + PS-MS–fed mice compared with HFD-fed mice. (Figure 4N–R).

Effects of Antibiotic-Induced Deletion of Gut Flora on Measures of Intestinal Integrity and Inflammation in Mice Exposed to ND or HFD with and without PS-MS in Drinking Water for 8 Wk

The number of goblet cells, *Muc2* mRNA and Muc2 protein levels were not significantly different between mice exposed to PS-MS in both diet groups with depleted microbiota (Figure 5A–C). ABX-treated mice also exhibited similar mRNA expression levels of *Tjp1* in colon tissues between the groups fed ND and ND + PS-MS, as well as between the groups fed a HFD and HFD + PS-MS. (Figure 5D). In addition, immunofluorescence results indicated that there were no significant differences in the protein expression

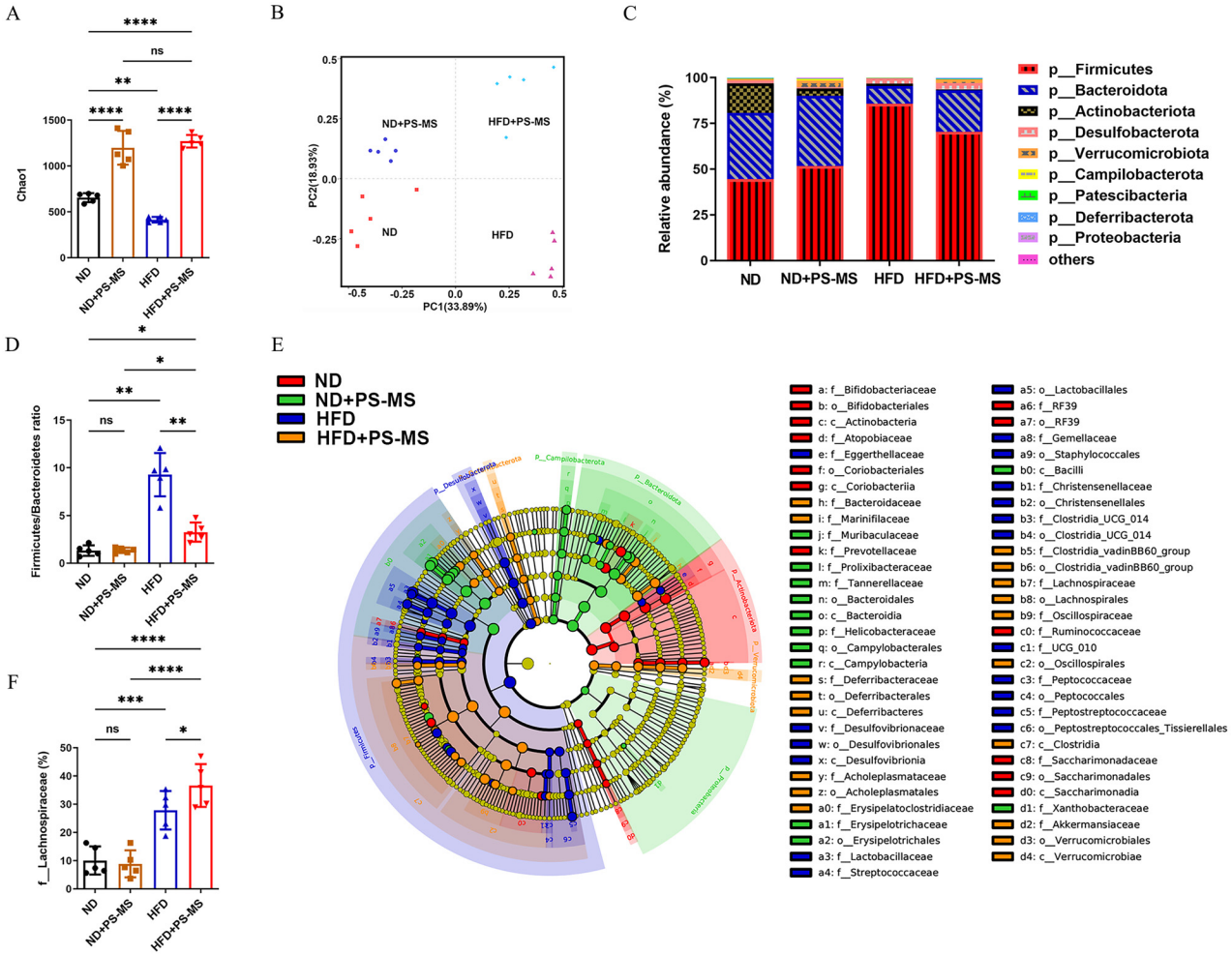

Figure 2. Composition of gut microbes in fecal samples from mice exposed to ND or HFD with and without PS-MS in drinking water for 8 wk. The fecal microbiota communities in ND- and HFD-fed mice treated with or without PS-MS for 8 wk were analyzed by 16S rRNA sequencing. (A) Chao1 index. (B) PCA plot based on OTUs. (C) Microbiota composition analysis at the phylum level. (D) The ratio of Firmicutes to Bacteroidetes. (E) LEfSe analysis of differential species abundance. (F–K) Relative abundances of *Lachnospiraceae*, *Oscillospiraceae*, *Bifidobacteriaceae*, *Marinifilaceae*, *Akkermansiaceae*, and *Atopobiaceae* at the family level. (L–N) Relative abundances of *Desulfovibrio*, *Bifidobacterium*, *Parabacteroides* at the genus level. Data of (H,J,K,M,N) were analyzed using the Brown–Forsythe and Welch ANOVA test. Data were determined using one-way ANOVA with a Tukey multiple comparison test. Data are represented as mean ± SD with scatter plots ($n = 5$). Each dot represents one mouse. Corresponding numeric data can be found in Table S3. The 16S rRNA raw reads are available at National Center for Biotechnology Information Sequence Read Archive repository (BioProject PRJNA990701). Note: ANOVA, analysis of variance; HFD, high-fat diet; LEfSe, LDA coupled with effect size measurements; PCA, principal component analysis; PS-MS, polystyrene microspheres; ND, normal diet; OTUs, operational taxonomic units; SD, standard deviation. $^{*}p < 0.05$, $^{**}p < 0.01$, $^{***}p < 0.001$, $^{****}p < 0.0001$.

levels of Tjp1 and occludin between the ND and ND + PS groups, as well as HFD and HFD + PS-MS groups in distal colon (Figure 5E–G). Interestingly, it is noteworthy that the differences in inflammatory factors in serum between the HFD + PS-MS and HFD groups, as well as those between HFD + PS-MS and ND groups observed in mice not exposed to antibiotics (i.e., ABX), were not seen in the ABX-exposed mice (Figure 5H–K).

Effects of Gut Microbiota from HFD + PS-MS Donor Group on Outcomes Related to Obesity and Metabolism in the Microbiota-Depleted HFD-Fed Recipient Mice for 8 Wk

To further investigate the impact of gut microbiota on PS-MS–associated outcomes, we conducted a FMT experiment. Microbiota from both the PS-MS + HFD group and HFD group were transferred to recipient mice pretreated with ABX, a mixture of antibiotics (vancomycin, neomycin sulfate, metronidazole, and ampicillin),[49] in their drinking water for 1 wk prior to FMT. The recipient mice were fed with a HFD, and obesity-related traits were assessed (Figure 6A). 16S rRNA gene profiling of transplant recipient fecal samples showed that recipient mice were successfully colonized with the donor microbiota. R-HFD and R-HFD + PS-MS mice assumed a phylogenetically similar composition to that of their respective donors as confirmed by PCA based on OTUs (Figure S5). After 8 wk of colonization, the recipient mice (R-HFD + PS-MS group) that received microbiota from the PS-MS + HFD donor group exhibited significantly greater BW compared with the recipient mice (R-HFD group) that received microbiota from the HFD donor group (Figure 6B,C). There was no significant difference in daily food intake and energy intake between the R-HFD + PS-MS and R-HFD groups (Figure 6D). The recipient mice in the R-HFD + PS-MS group exhibited greater liver weight, MASLD score, white adipose tissue mass (iWAT, eWAT, pWAT), average inguinal adipose tissue area, and serum lipid concentrations (serum TC, LDL-C, and LDL-C/HDH-C) (Figure 6E–L,N,O). Notably, fasting blood glucose concentrations in the R-HFD + PS-MS group were higher than the R-HFD group; however, there was no significant difference in blood glucose

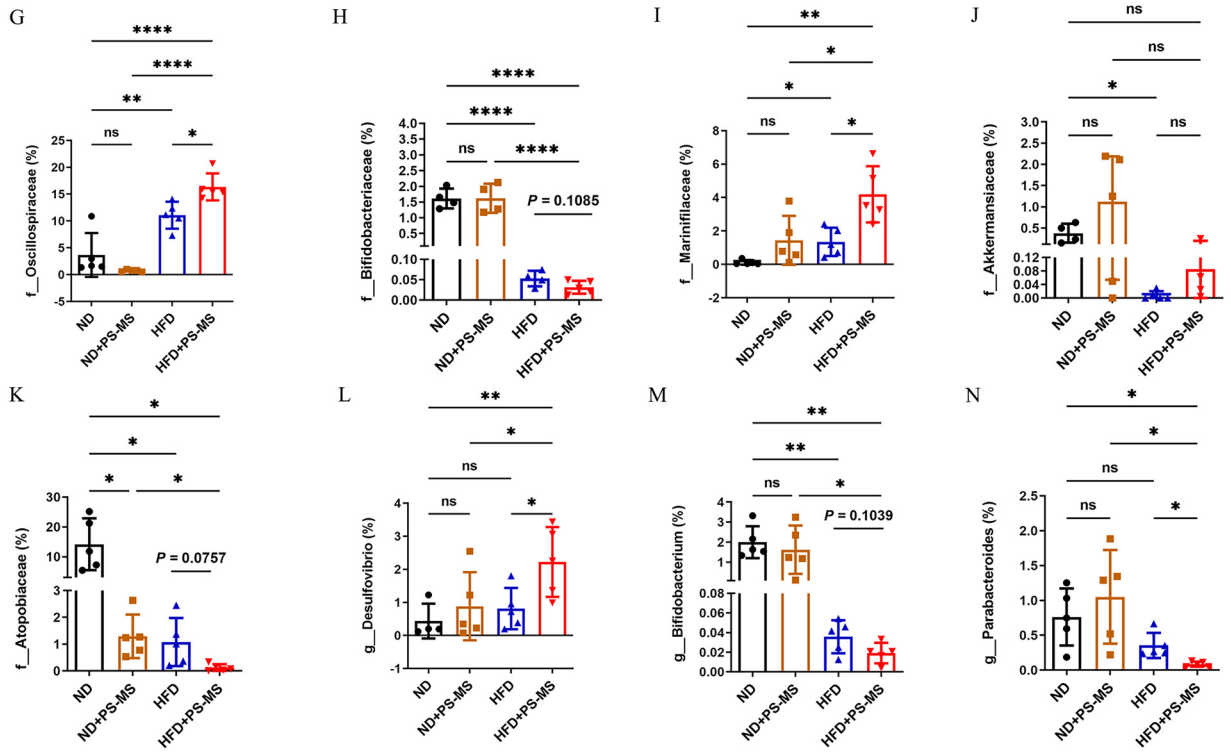

Figure 2. (*Continued.*)

AUC between the R-HFD group and the R-HFD + PS-MS group (Figure 6M).

Effects of Gut Microbiota from HFD + PS-MS Donor Group on MUC2 and Tjp1 Expression and Inflammatory Cytokines in Microbiota-Depleted, HFD-Fed Recipient Mice for 8 Wk

Remarkably, recipient mice of the fecal bacterial solution obtained from the HFD + PS-MS group exhibited fewer goblet cells, lower protein expression of MUC2 and relative mRNA levels of *Muc2* and *Tjp1* in colon tissues, compared with those receiving the fecal bacterial solution from the HFD group (Figure 7A–D). Moreover, we observed higher levels of inflammatory cytokines, including TNF-α and IL-17A, in the serum of mice from the R-HFD + PS-MS group compared with R-HFD group. However, no difference was found for IL-6 ($p = 0.086$). (Figure 7E–G).

Discussion

MPs are omnipresent in our environment.[14] Recent scientific investigations have increasingly substantiated the existence of MPs within the human body, raising concerns about their potential hazards.[18–20] However, the impact of PS-MS on obesity of humans remains unclear. Considering that HFD can lead to obesity, and that the co-occurrence of HFD and PS-MS might exacerbate the condition of obesity, in this study our aim was to investigate the obesogenic effects of PS-MS and elucidate the underlying mechanisms when PS-MS were administered via drinking water in a model of obesity induced by a HFD. Our study presented compelling evidence that PS-MS exacerbated HFD-induced obesity (8-wk HFD) and promoted weight gain, which was associated with impaired glucose and lipid metabolism. Because a considerable proportion of ingested 5-μm PS-MS traversed the gastrointestinal tract of C57BL/6 J mice following 28 d of 5-μm PS-MS exposure via oral gavage,[32] we hypothesized that the gut microbiota and epithelial barrier may represent novel targets for PS-MS toxicity, particularly in obese populations. By using a mouse model of obesity induced by a HFD, and employing ABX treatment and FMT, this study has furnished compelling evidence that PS-MS treatment can induce inflammation and obesity by altering the composition of the gut microbiota and compromising MUC2 expression of the distal colon. To our best knowledge, this is the first study to explore the obesity-enhancing effects of the combination of a HFD and PS-MS, as well as to evaluate the role of PS-MS–induced alterations of gut microbiota in HFD-induced obesity. Our findings suggest that PS-MS microspheres might exacerbate Western diet–induced obesity and related metabolic disorders in humans and that the gut microbiota is a crucial target for the obesity-promoting effects of PS-MS.

The daily intake of MPs is still uncertain, despite organisms being constantly exposed to them. This is particularly true for humans, because the pathways of MPs contact are diverse and complex, leading to varying assessments of body intake. The dose selection for PS-MS took into account both their toxicological and environmental significance. PS-MS with a size of 5 μm and a toxic effect were chosen as exposure materials on the basis of previous studies on intestinal toxicity in mice using a range of 5 μg/d to 1 mg/d.[31,50–52] In terms of environmental significance, on average, humans could potentially ingest 0.1–5 g of MPs/wk globally.[53] Based on the weight of the mice, which was ∼20 g, their daily intake of PS-MS was calculated to range between 37.14 μg/d and 1.86 mg/d. It was estimated that each control mouse consumed 3.6 mL of water/d in this study, resulting in a PS-MS intake of 36 μg/d per mouse. The intake of PS-MS in mice is equivalent to the minimum potential exposure dose for humans (0.1 g of MPs/wk).[53] The mice were exposed daily to PS-MS through their drinking water, simulating the major route of MPs exposure in mammals.[54,55] Therefore, the selected doses were of environmental and toxicological significance.

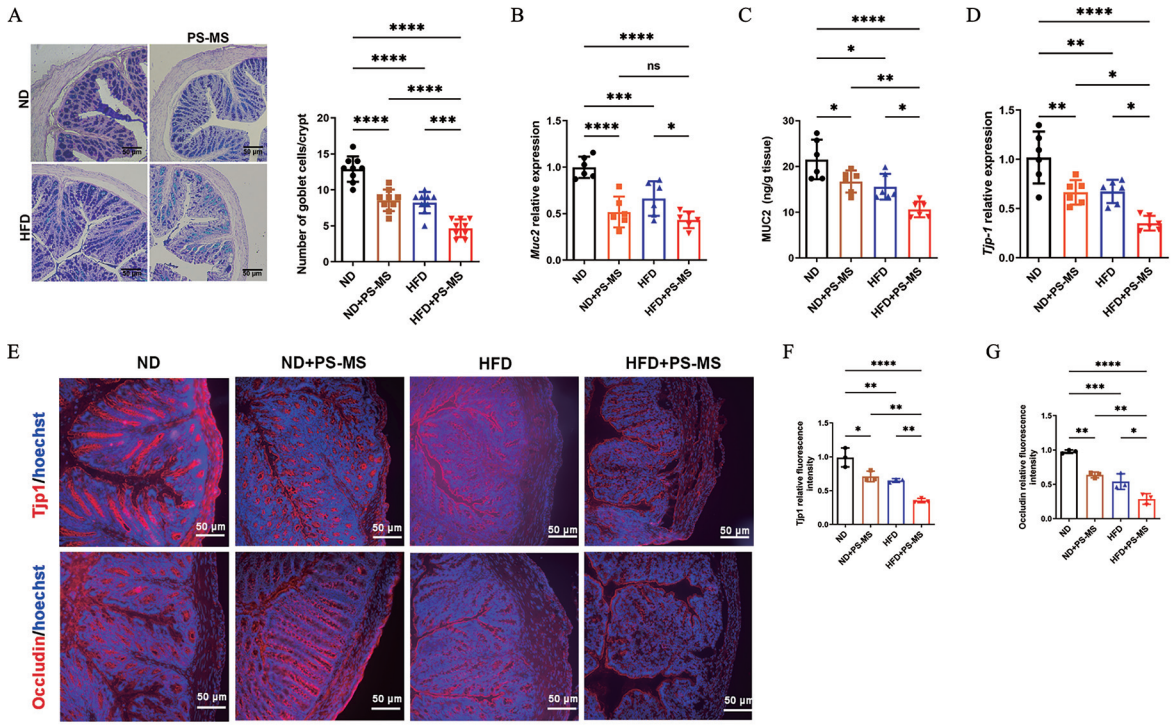

Figure 3. Muc-2, Tjp1, and occludin expression and measures of inflammatory cytokines in mice exposed to ND or HFD with and without PS-MS in drinking water for 8 wk. (A) Alcian blue/periodic acid-Schiff (AB/PAS) staining and quantification of goblet cell numbers from sections of distal colon stained with AB/PAS. (B) *Muc2* relative expression levels in colon tissue. (C) MUC2 protein contents in colon tissue. (D) *Tjp1* relative expression levels in colon tissue. (E) Representative immunofluorescence staining of Tjp1 and Occludin protein of distal colon; quantification of (E) is shown in (F) and (G) ($n = 3$); each dot on the graph represents one mouse. (H) LPS, (I) TNF-α, (J) IL-6, (K) IL-1β, and (L) IL-17A concentrations in serum. (M) The correlation of the 15 top family of gut microbiota differences with clinical parameters related to obesity presented as a heat map analysis. Pearson correlation values were used for the matrix, with red indicating a positive correlation and blue indicating a negative correlation. Data were determined using one-way ANOVA with a Tukey multiple comparison test. Data are represented as mean ± SD in scatter plots ($n = 6$ unless otherwise indicated). Corresponding numeric data can be found in Table S3. Note: ANOVA, analysis of variance; eWAT, epididymal adipose tissue; HDL-C, high-density lipoprotein cholesterol; HFD, high-fat diet; IL, interleukin; iWAT, inguinal white adipose tissue; LDL-C, low-density lipoprotein cholesterol; LPS, lipopolysaccharide; ND, normal diet; ns, nonsignificant; PS-MS, polystyrene microspheres; pWAT, perirenal white adipose tissue; SD, standard deviation; TC, total cholesterol; TG, triglycerides; TNF, tumor necrosis factor. $^{*}p < 0.05$, $^{**}p < 0.01$, $^{***}p < 0.001$, $^{****}p < 0.0001$.

Recently, it has been discovered that MPs have the ability to disrupt glucose and lipid metabolism in mice[56]; however, the role of PS-MS in obesity populations is not yet well understood. Our study first suggested that PS-MS exacerbated HFD-induced obesity (as determined by greater weight gain, higher lipid levels, and more adipose mass in HFD + PS-MS vs. HFD mice). It was noteworthy that the lipid accumulation in the liver and white adipose tissue after PS-MS exposure was more pronounced in HFD-fed mice but not in ND-fed mice, which suggested that certain susceptible populations might be more affected by the impact of PS-MS. This suggested that PS-MS–induced obesity was related to diet. This could be attributed to the fact that, in addition to PS-MS consumption, HFD also was associated with mucosal damage and low-grade inflammation in mice.[57] It is well known that overweight and obesity are associated with significant changes in metabolism in mice, especially glucose and lipid metabolism.[58] We consistently found that glucose tolerance was severely impaired in the HFD + PS-MS group and that serum levels of TC and LDL-C and the LDL/HDL-C ratio were significantly higher. Together, our results suggest that alterations in glucose and lipid metabolism played a significant role in the development of PS-MS–induced obesity. One recent study revealed that the development of obesity in mice exposed to PS-MS was effectively dose-controlled under ND conditions.[59] Specifically, relatively low doses of PS-MS were found to trigger obesity, whereas higher doses did not. In line with these observations, we report that administering 10-mg/L PS-MS in drinking water did not induce obesity in mice on a ND. Intriguingly, and in contrast to the above findings, we observed that 10-mg/L PS-MS exposure promoted fat accumulation in mice fed a HFD, suggesting that PS-MS–induced obesity was highly influenced by diets as well as dosage of PS-MS. Previous studies have reported that oral intake of 0.45–0.53 μm PS-COOH (Polystyrene-carboxylic acid) beads or a combination of PS-MS with varying particle sizes (5, 50, 100, and 200 μm) led to a reduction weight in HFD-fed mice.[60,61] This implies that PS-MS with distinct particle sizes and properties may have dissimilar effects on BW. In the following phase, we will investigate the impact of PS-MS and other microplastic particles on obesity in mice under varying dietary conditions and dosage levels. Our findings demonstrate that exposure to PS-MS at levels below those typically encountered by humans worsened HFD-induced obesity in mice, potentially elucidating the link between increased plastic production and the growing global prevalence of obesity.

Recent studies have shown that PS-MS–induced obesity is related to gut microbiota.[33,59] The Chao1 index is frequently employed in ecology for estimating the total number of species. However, the Shannon's diversity measure is commonly used in ecology for estimating community diversity. Our study reveals that the administration of PS-MS resulted in a significant increase in the Chao1 index of the gut microbiota in both the ND and HFD diet groups. Intriguingly, no significant difference was observed in the Shannon's index among the ND, ND + PS, and HFD groups. This observation suggests that the influence of ND + PS or HFD on the gut microbiota may primarily affect its abundance rather than its diversity. Previous research has revealed

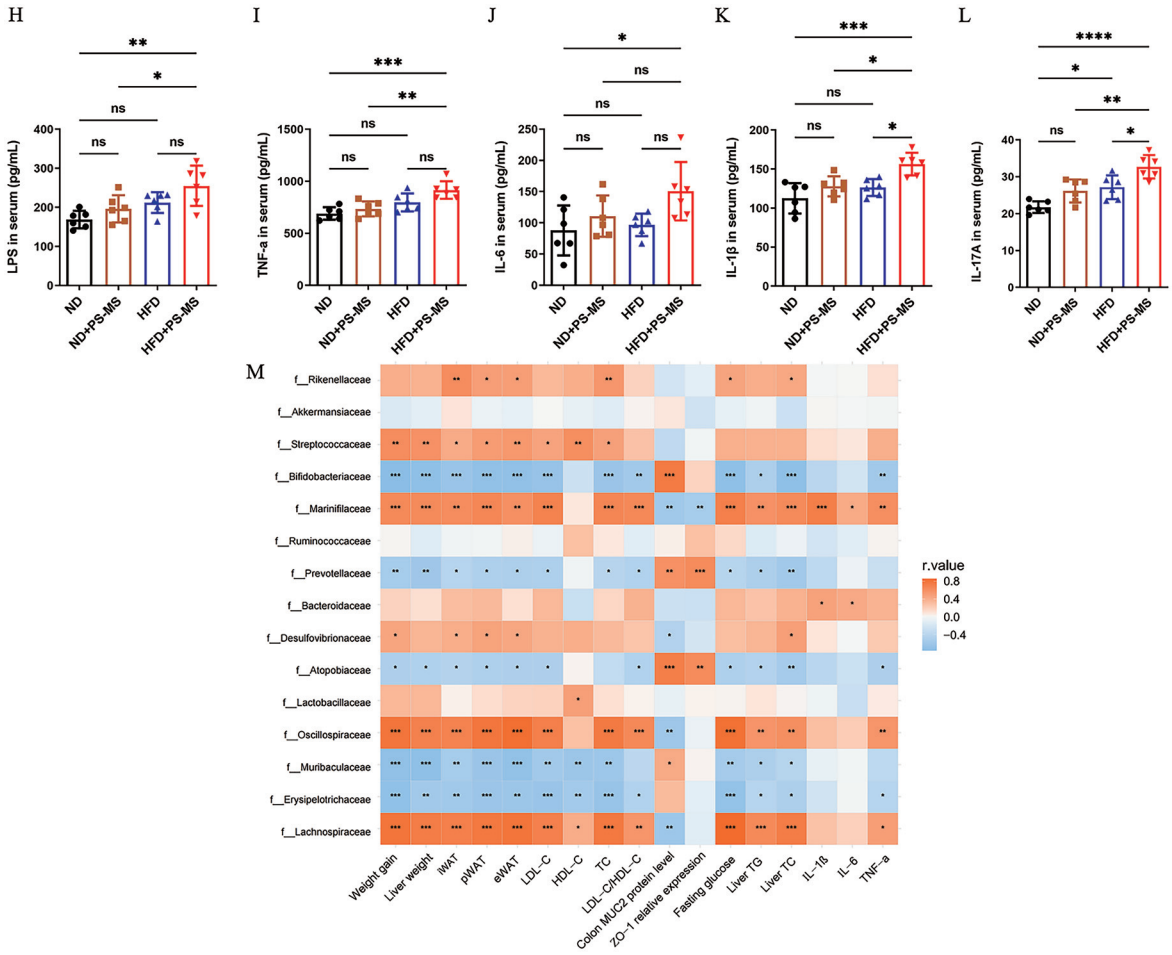

Figure 3. (*Continued.*)

that obese mice have different intestinal compartments compared with their normal counterparts, with a higher proportion of *Firmicutes* phylum.[62,63] In addition, it has been suggested that *Firmicutes* phylum may be implicated in obesity, given that a larger population of these microorganisms can effectively convert food to energy at accelerated rates.[64] This study found that PS-exposed mice had a greater relative abundance of the class Clostridia (phylum *Firmicutes*), including family *Lachnospiraceae*, and *Oscillospiraceae* in the HFD + PS-MS group. Interestingly, PS-MS–exposed mice also exhibited a lower F:B ratio, which is considered a key marker of diet-induced obesity.[10,11] These findings suggest that PS-MS can modify the population of certain bacteria within the *Firmicutes* phylum, leading to obesity independent of the F:B ratio.

Therefore, we hypothesize that the relative abundance alterations of certain family levels within the *Firmicutes* bacteria was a significant factor in PS-MS–induced obesity. Previous studies have reported an relative abundance increase of family *Lachnospiraceae* in both mice and humans with obesity and diabetes.[65,66] Mechanistic research has shown that *Fusimonas intestini*, a commensal species of *Lachnospiraceae*, contributed to diet-induced obesity by producing excessive long-chain fatty acids in mice.[67] In our study, *Lachnospiraceae* was the predominant family of *Firmicutes*, comprising nearly 40% of the total population. The overproduction of long-chain fatty acids could potentially be linked to PS-MS–induced obesity. Family *Oscillospiraceae* was reported to be increased in HFD-fed mice. This family exhibited a positive correlation with obesity indexes, bacterial translocation parameters, blood parameters, pro-inflammatory cytokine, energy metabolism, Toll-like receptor 4/Nuclear factor-kappa B (TLR4/NF-κB) pathways, and colonic permeability.[68,69] Consistent with these observations, mice exposed to PS-MS had a significantly greater percentage of family *Oscillospiraceae* in the gut microbiota of the HFD + PS-MS group (compared with HFD). In addition to alterations in bacterial abundance within the *Firmicutes* phylum, there was a remarkably greater relative abundance of the family *Marinifilaceae* in HFD + PS-MS group, which were significantly associated with visceral fat and body fat percentage in a small cohort of children.[70] In our mouse study, the relative abundance of family *Lachnospiraceae*, *Oscillospiraceae*, and *Marinifilaceae* were significantly positively correlated with obesity-related indicators.

In particular, the relative abundance of genus *Akkermansia* was higher in the HFD + PS-MS treatment group. Recent research has highlighted the significance of genus *Akkermansia* as an essential functional bacterium that regulates human immunity and metabolism in the intestine, significantly linked with human health and diseases.[71,72] Normally, the typical colonization pattern of the genus *Akkermansia* involves inhabiting the outer mucous layer of the gastrointestinal tract, playing a crucial role in regulating mucin production and preserving the integrity of the mucus layer.[73] In addition, *Akkermansia* has shown significant potential in ameliorating metabolic endotoxemia, insulin resistance, adipose tissue accumulation, and fasting hyperglycemia in mice with diet-induced obesity.[74] Nevertheless, there is ongoing debate surrounding the involvement of the genus *Akkermansia* in intestinal disorders. Several studies

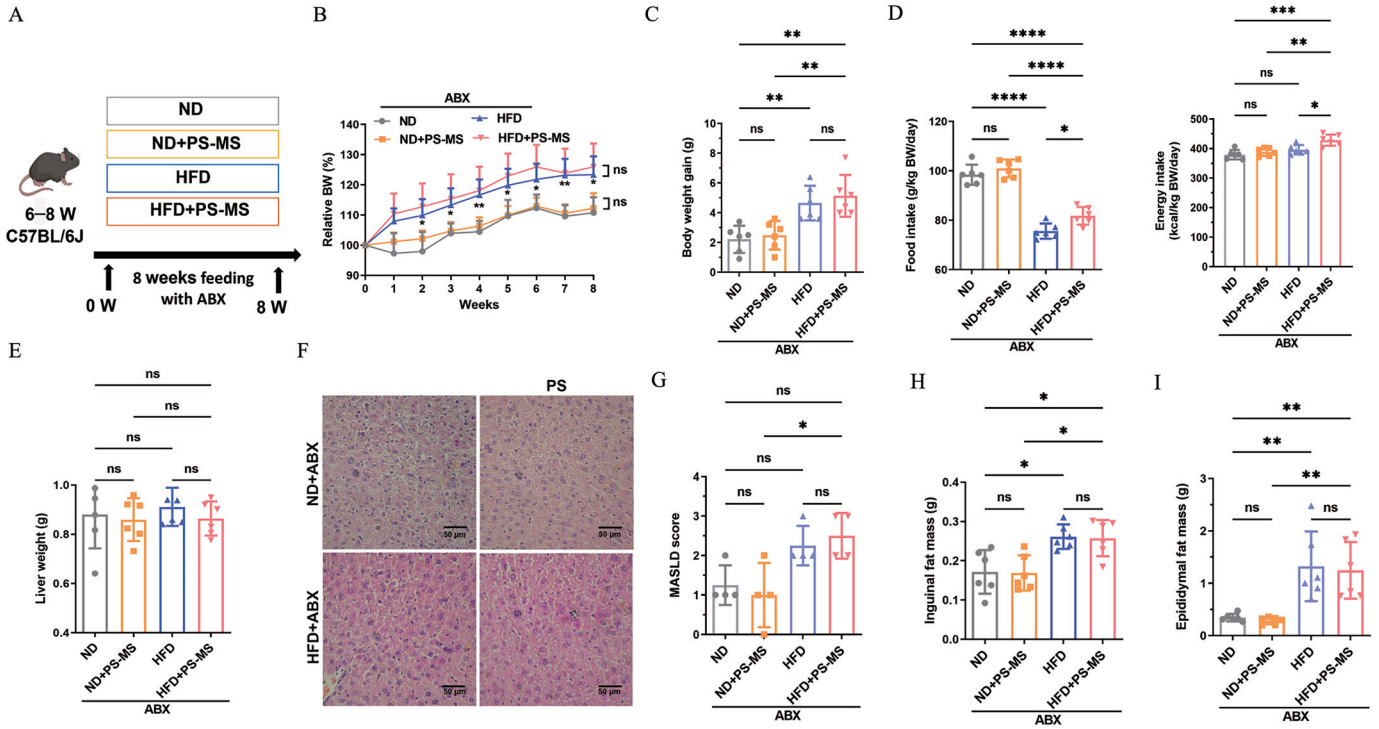

Figure 4. Effect of antibiotic-induced deletion of gut microflora on measures related to obesity and metabolism in mice exposed to ND or HFD with and without PS-MS in drinking water for 8 wk. The ND- and HFD-fed mice were administrated PS-MS in drinking water and given ABX [penicillin (100 mg/kg BW), neomycin (100 mg/kg BW), metronidazole (100 mg/kg BW), and vancomycin (50 mg/kg BW)] by gavage daily for 8 wk. (A) The mice fed a ND or HFD ± PS were treated with ABX starting at 8 wk of age. (B) Relative BW calculated as follows: BW/primary BW. Data were determined using two-way repeated measures ANOVA with a Tukey multiple comparison test for individual time points. (C) BW gain calculated as follows: weight after 8 wk of treatment – primary BW (D) Food intake and energy intake. (E) Liver weight. (F) Representative microscopic observation of livers tissue by H&E staining. (G) MASLD histological activity score ($n = 4$); each dot on the graph represents one mouse. Mass of (H) inguinal adipose tissue, (I) epididymal adipose tissue, and (J) perirenal adipose tissue. (K) Representative microscopic observation of adipocyte size of inguinal adipose tissue. (L) Quantification of mean inguinal adipose tissue area. Each dot on the graph represents one mouse. (M) Fasting blood glucose level and area under the curve (AUC) of blood glucose levels. Serum (N) TC, (O) TG, (P) LDL-C, and (Q) HDL-C levels and (R) fold changes of LDL-C/HDL-C measured with the corresponding assay kits. All values are represented as mean ± SD in scatter plots ($n = 6$ unless otherwise indicated). Each dot represents one mouse. Data were determined using one-way ANOVA with a Tukey multiple comparison test. Corresponding numeric data can be found in Table S3. Note: ABX, antibiotic cocktail; ANOVA, analysis of variance; BW, body weight; H&E, hematoxylin and eosin; HDL-C, high-density lipoprotein cholesterol; HFD, high-fat diet; LDL-C, low-density lipoprotein cholesterol; MASLD, metabolic dysfunction-associated steatotic liver disease; ND, normal diet; ns, non-significant; PS-MS, polystyrene microspheres; SD, standard deviation; TC, total cholesterol; TG, total triglycerides. For (B), $^{*}p < 0.05$; $^{**}p < 0.01$, ND vs. HFD. For (C,D,G–L), $^{*}p < 0.05$, $^{**}p < 0.01$, $^{***}p < 0.001$, $^{****}p < 0.0001$.

have indicated a potential beneficial effect of *Akkermansia* in mitigating obesity and its associated metabolic syndrome in murine models.[74,75] In contrast, clinical studies have revealed a high frequency of genus *Akkermansia* in the fecal matter of infants with eczema. Moreover, it was shown that genus *Akkermansia* was associated with gut barrier integrity and greater risk for eczema in infants.[76] Recently, a study demonstrated that a high-sugar diet could augment the relative abundance of genus *Akkermansia* in mice. This was associated with the destruction of the intestinal barrier function, leading to colitis via stimulating the activity of mucolytic enzymes within the microbiota.[77] In this study, PS-MS–exposed mice exhibited a higher relative abundance of the *Akkermansia* family and lower MUC2 expression levels in the colon tissue of HFD-fed mice, which potentially contributed to the worsening of obesity.

Numerous reports have suggested that the onset of obesity induced by dietary factors is linked to changes in gut microbiota, characterized by a reduction in beneficial microbial genera, which ultimately contributes to obesity and metabolic syndrome.[78–80] Consistently, our study also revealed a lower abundance of beneficial bacteria in PS-MS–exposed mice fed a HFD, including family *Atopobiaceae* and genus *Bifidobacterium*, as well as genus *Parabacteroides*. The function of family *Atopobiaceae* is not yet fully understood; however, previous studies have reported a significant decrease in the abundance of family *Atopobiaceae* in HFD-induced diabetic mice.[81] Consistent with the findings of this study, the relative abundance of family *Atopobiaceae* was observed to be negatively correlated with the obesity index induced by PS-MS, indicating a potential role of family *Atopobiaceae* in anti-obesity. Previously, the *Bifidobacterium* spp. was associated with less obesity in rats,[82] which was negatively related to intestinal permeability, metabolic endotoxemia, and low-grade inflammation.[83,84] Similarly, the present study observed the lower relative abundance of the genus *Bifidobacterium* in PS-MS + HFD-fed mice compared with HFD-fed mice, which was a negatively correlated with obesity-related indicators. Except for genus *Bifidobacterium*, a study revealed that *Parabacteroides goldsteinii* was identified as a key contributor to the anti-obesity effects.[85] We found that PS-MS–supplemented mice exhibited a lower abundance of genus *Parabacteroides* in mice fed a HFD, indicating that the supplementation of *Parabacteroides* spp. might be another effective approach to alleviate the adverse health effects induced by PS-MS. Further research is necessary to gain a better understanding of the potential therapeutic applications of *Bifidobacterium* spp. and *Parabacteroides* spp. in managing PS-MS–induced obesity and related metabolic disorders. Taken together, we conclude that microbial dysbiosis is likely associated with PS-MS–induced obesity in mice.

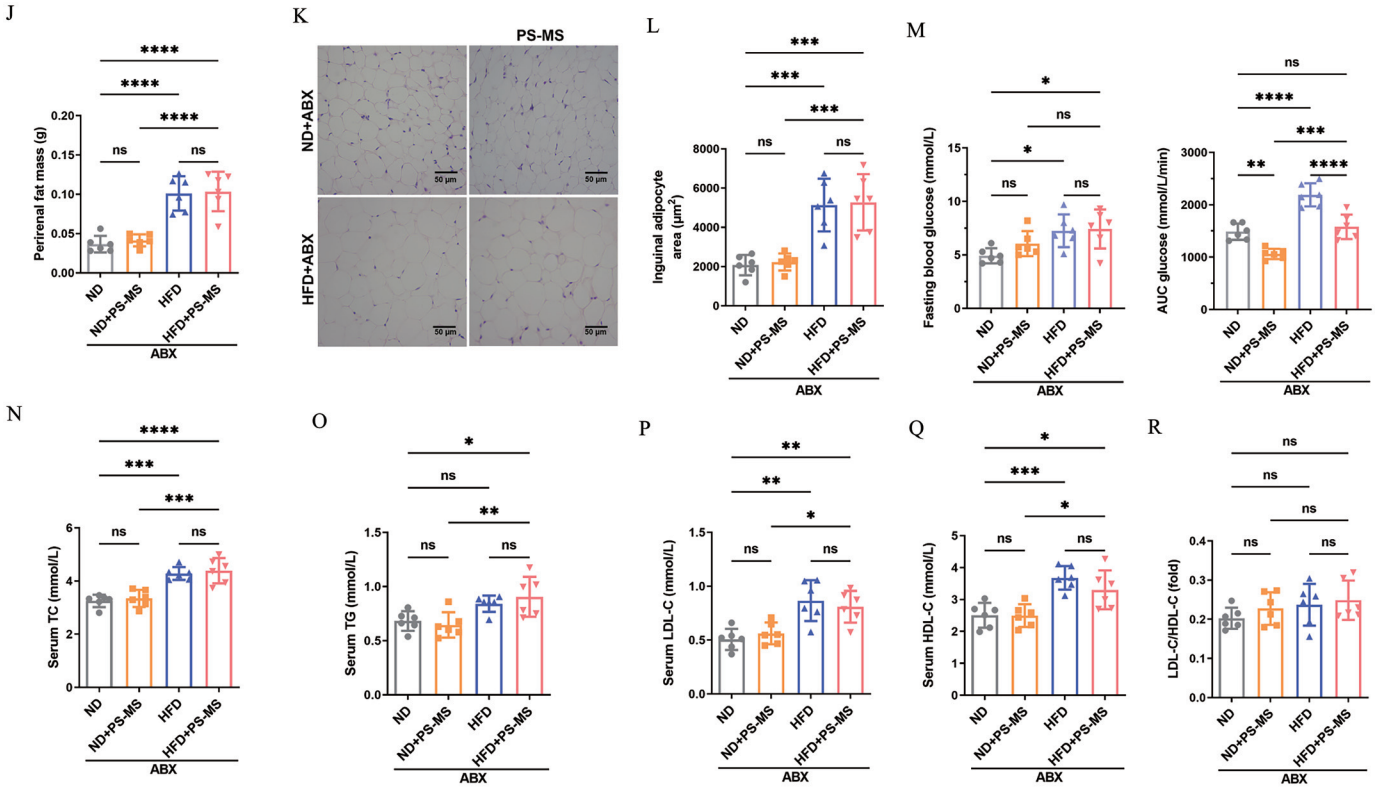

Figure 4. (*Continued.*)

HFD has been observed to induce alterations in the composition of gut microbiota, leading to significant reduction in the thickness of the intestinal mucus layer.[74] The mucus layer, which is formed by mucin proteins and hydrated gel with glycosylation, plays an essential role in separating the intestinal epithelium from its contents.[86] The integrity of the intestinal mucosal barrier plays a crucial role in safeguarding human health by preventing direct interaction between microorganisms and epithelial cells. Impairment of this barrier has been implicated in the pathogenesis of various diseases, including inflammatory bowel disease,[87] and metabolic diseases.[88] Therefore, we hypothesized that PS-MS–induced microbial dysbiosis exacerbated mucosal layer injury. This study discovered that PS-MS–exposed mice had lower expression of mucus-specific mRNA including *Muc2* and tight junction-related *Tjp1* in HFD-fed mice. Consistently, the expression levels of MUC2 and TJP1 were also lower. A study has shown that a HFD affects the expression of the housekeeping gene *Gapdh* in liver and adipose tissues.[89] However, it remains unclear whether a HFD affects the expression of *Gapdh* in the intestine. Although this experiment did not employ different housekeeping genes for verification, the results have been validated at both the gene and protein levels, thereby ensuring the integrity of the experimental process.

Destruction of the mucus layer can select and enrich certain bacteria like *Lachnospiraceae*, which reside in the interfold regions of the colon, promoting direct contact of the bacteria with the intestinal epithelium, thus initiating inflammation.[90] A previous study showed that PS-MS–exposed mice exhibited greater inflammatory markers and insulin resistance.[60] Further correlation analysis also showed that the expression levels of MUC2 were negatively correlated with the abundance of *Lachnospiraceae*. Based on these results, we speculated that PS-MS impaired the integrity of intestinal barrier, which allows LPS entry into the systemic circulation, thereby triggering inflammation. This hypothesis was supported by elevated serum levels of LPS and pro-inflammatory cytokines (TNF-α, IL-17A, IL-1β, and IL-6). Furthermore, correlation analysis also revealed significant associations between the dysregulated gut microbiota induced by PS-MS and indicators related to obesity and MUC2 expression levels, as well as inflammatory factors. Our findings suggest that PS-induced dysbiosis disrupted the gut microbiota, leading to increased penetration of toxic gut molecules into the body via impaired intestinal barrier in HFD-fed mice. These findings provide further evidence for the role of PS-MS–induced microbial imbalance in perpetuating metabolic dysfunction, and highlight the potential utility of targeting the gut microbiota as a therapeutic strategy for treating obesity and associated disorders.

To further investigate the role of gut microbiota in obesity induced by PS-MS, we conducted a correlation analysis between the relative abundance of PS-associated gut microbiota and obesity-related indicators using Spearman's correlation. Overall, we found that *Lachnospiraceae*, *Oscillospiraceae*, and *Marinifilaceae* showed positive correlations with BW, liver weight, mass of white adipose tissue, fasting blood glucose, and serum lipid concentrations (LDL-C, TC), as well as liver lipid concentrations (TG, TC), and pro-inflammatory cytokines (IL-1β, IL-6, TNF-α, IL-17A) in the serum. Conversely, they were negatively correlated with the MUC2 protein level in the distal colon. On the other hand, *Bifidobacteriaceae* and *Atopobiaceae* displayed the opposite trend. These findings suggest that PS-MS administration effectively altered the gut microbiota induced by a HFD in mice and subsequently promoted obesity-related indicators.

Alongside germ-free animal models, antibiotic-treated animal models are frequently employed in the investigation of intestinal bacteria.[91] To verify whether the adverse effect of PS-MS on obesity was mediated by the intestinal flora, In this study, a combination of four broad-spectrum antibiotics—namely penicillin, neomycin, metronidazole, and vancomycin—were simultaneously administered for 8 wk, resulting in a 97% reduction of commensal bacteria within murine intestinal microbiota. Mice treated with the ABX

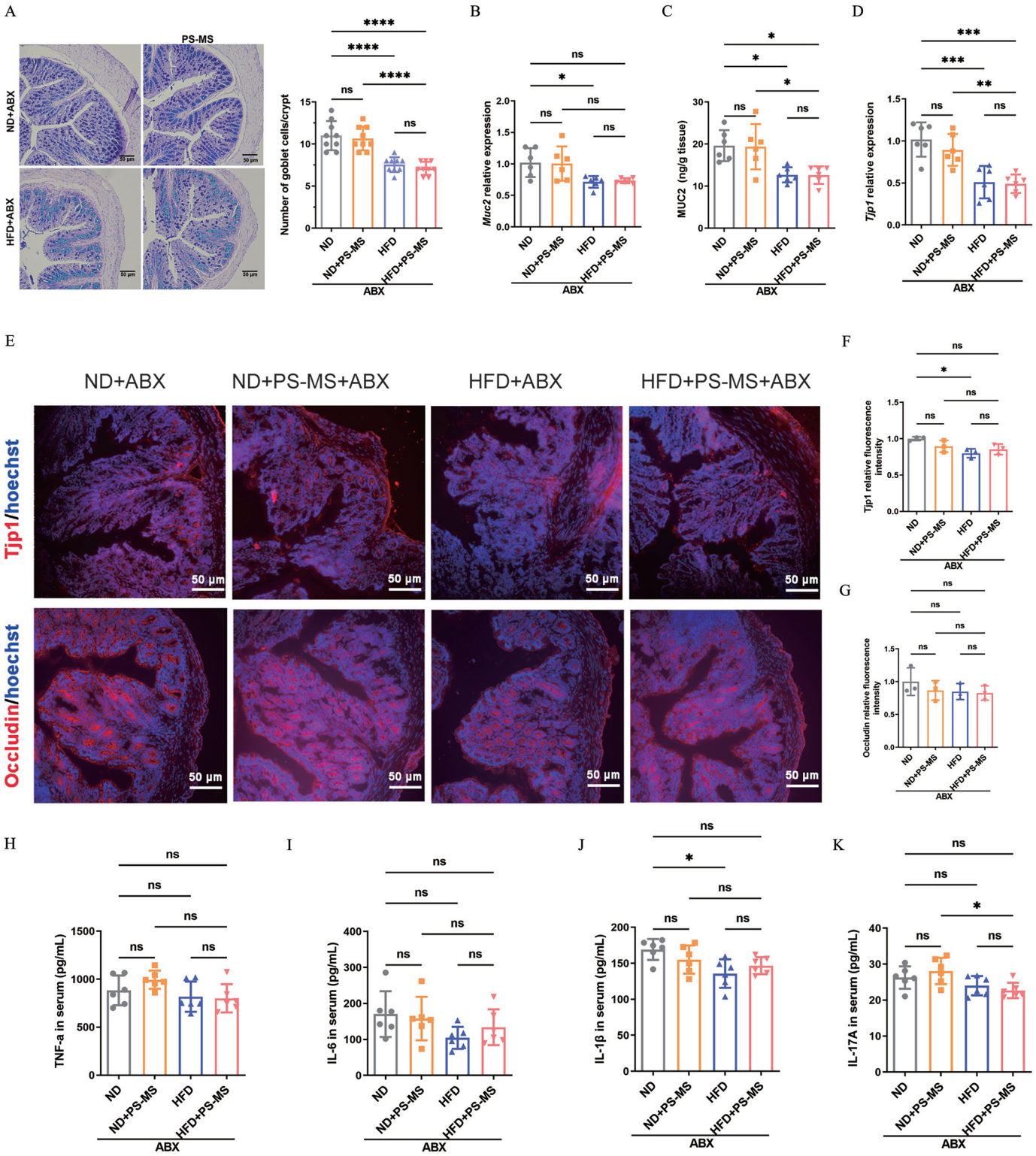

Figure 5. Effects of antibiotic-induced deletion of gut flora on Muc2 and Tjp1 expression and inflammatory cytokine expression in mice exposed to ND or HFD with and without PS-MS in drinking water for 8 wk. (A) Alcian blue/periodic acid-Schiff (AB/PAS) staining of distal colon, and quantification of goblet cell numbers from colonic sections stained with AB/PAS. Each data represents 1 crypt, 3 slices/group, 3 crypts/slice ($n = 9$). (B) MUC2 protein contents in colon tissue. (C) *Muc2* relative expression levels in colon tissue. (D) *Tjp1* relative expression levels in colon tissue. (E) Representative immunofluorescence staining of Tjp1 and occludin protein of distal colon. Quantification of (E) is shown in (F) and (G) ($n = 3$); each dot on the graph represents one mouse. The (H) TNF-α, (I) IL-6, (J) IL-1β, and (K) IL-17A concentrations in serum samples detected by ELISA. Data were determined using one-way ANOVA with a Tukey multiple comparison test. Data are represented as mean ± SD in scatter plots ($n = 6$ unless otherwise noted). Corresponding numeric data can be found in Table S3. Note: ABX, antibiotic cocktail; ANOVA, analysis of variance; ELISA, enzyme-linked immunosorbent assay; HFD, high-fat diet; IL, interleukin; ND, normal diet; ns, nonsignificant; PS-MS, polystyrene microspheres; SD, standard deviation; TNF, tumor necrosis factor. $^{*}p < 0.05$, $^{**}p < 0.01$, $^{***}p < 0.001$, $^{****}p < 0.0001$.

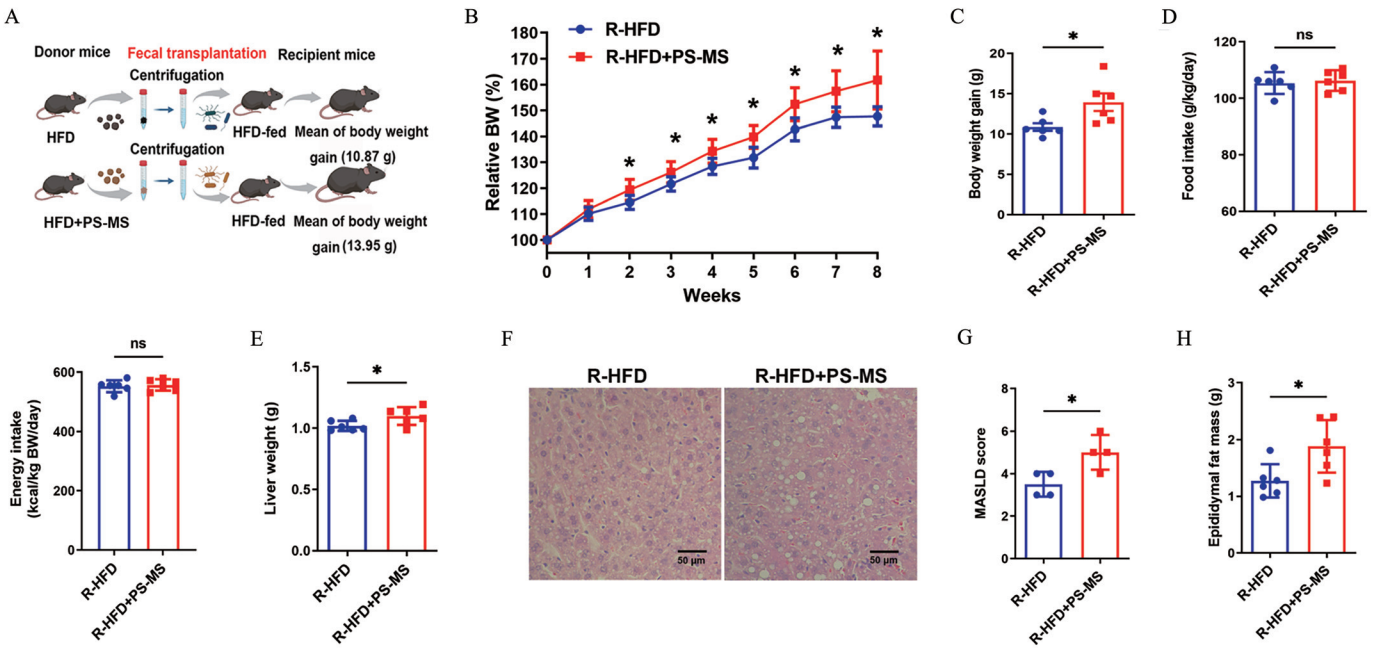

Figure 6. Effect of gut microbiota from the HFD + PS-MS donor group on outcomes related to obesity and metabolism in the microbiota-depleted HFD-fed recipient mice for 8 wk. The mice were randomly divided into four groups ($n = 6$). Before FMT, the mice were given an antibiotic cocktail for 1 wk. HFD-fed mice were given normal water (HFD group) or water containing PS-MS at 10 mg/L (HFD + PS-MS group). The recipients of the horizontal fecal transfer from HFD mice are referred to as HFD receivers (R-HFD). The recipients of the horizontal fecal transfer from PS-MS–treated mice are referred to as HFD + PS-MS receivers (R-HFD + PS-MS). (A) Study design of fecal transplant experiment. (B) Relative BW calculated as follows: BW/primary BW. Data were tested with multiple unpaired *t*-tests. (C) BW gain. (D) Food intake and energy intake. (E) Liver weight. (F) Representative microscopic observation of liver tissue by H&E staining. (G) MASLD histological activity score ($n = 4$). Each dot on the graph represents one mouse. Mass of (H) epididymal adipose tissue, (I) perirenal adipose tissue, and (J) inguinal adipose tissue. (K) Representative microscopic observation of adipocyte size of inguinal adipose tissue. (L) Statistical analysis of mean inguinal adipose tissue area. Each dot on the graph represents one mouse. (M) Fasting blood glucose level and area under the curve (AUC) of blood glucose levels. (N) TC (data of TC were analyzed using the Mann–Whitney test), LDL-C levels in serum (O) LDL-C/HDL-C ratio. All values are represented as mean ± SD in scatter plots ($n = 6$). Each dot represents one mouse. Unless otherwise specified, data were analyzed using Student's *t*-test for comparisons between two groups. Corresponding numeric data can be found in Table S3. Note: BW, body weight; FMT, fecal microbiota transplantation; H&E, hematoxylin and eosin; HDL-C, high-density lipoprotein cholesterol; HFD, high-fat diet; LDL-C, low-density lipoprotein cholesterol; MASLD, metabolic dysfunction-associated steatotic liver disease; ns, nonsignificant; PS-MS, polystyrene microspheres; R-HFD, HFD receivers; R-HFD + PS-MS, HFD + PS-MS receivers; SD, standard deviation; TC, total cholesterol; TG, total triglycerides. For (B), $^{*}p < 0.05$, R-HFD + PS-MS vs. R-HFD. For (C–E,G–J,L–O), $^{*}p < 0.05$, $^{**}p < 0.01$, $^{***}p < 0.001$.

exhibited no significant differences in obesity-related outcomes (weight gain, liver weight, adipose mass, and blood lipid levels) between PS-MS–exposed and control mice, thus supporting the hypothesis that gut microbiota play a crucial role in the development of this disorder. Interestingly, mice in the HFD + PS-MS group consumed more food; however, there was no significant variation in BW, potentially due to the absence of intestinal flora. The intestinal flora promotes the absorption of fat from the diet and therefore plays an important role in the development of obesity.[92] In the absence of microorganisms, proper overfeeding might not promote the absorption of fat, thereby mitigating the exacerbation of PS-MS–induced obesity. A more concerning result was that mice exposed to PS-MS demonstrated lower expression of MUC2, Tjp1, and occludin proteins in distal colon tissues, Interestingly, this lower expression depended on the presence of gut flora; when mice were treated with the ABX, the differential expression of MUC2, Tjp1, and occludin proteins between the ND and ND + PS-MS groups, as well as between the HFD and HFD + PS-MS groups, disappeared. Therefore, our results suggest that PS-MS–associated intestinal barrier outcomes may have been mediated via intestinal flora. However, this investigation had certain limitations, most notably our inability to fully eradicated the intestinal microbial population.

Intestinal dysbiosis may undermine the integrity of the intestinal barrier, facilitating the direct translocation of LPS into the circulatory system and thereby instigating a low-grade inflammatory response.[47] Our findings suggest that inflammation and obesity associated with PS-MS exposure is contingent upon the composition of the intestinal microbiota. Notably, we found that the genus *Desulfovibrio*, a sulfate-reducing bacteria, exhibited an greater abundance in the PS-MS + HFD group. This particular bacterium has been demonstrated to synthesize LPS, exhibiting endotoxin activity that is 1,000-fold higher than that of other gut bacteria.[93] We also found that family *Deferribacteres* was enriched at higher taxonomic levels such as phylum, class, and order in the HFD + PS-MS group. Mounting evidence suggests that family *Deferribacteres* was strongly associated with up-regulated pro-inflammatory cytokines and exacerbation of inflammation and obesity-induced metabolic disease type 2 diabetes.[94,95] Furthermore, we observed a decrease in the number of family *Bifidobacteriaceae* in the PS-MS + HFD group compared with the HFD alone group, which is known to have a negative correlation with intestinal permeability, metabolic endotoxemia, and low-grade inflammation.[96] Based on the outcomes of the ABX exposure, we propose that differences in gut microbiota significantly contributed to the lower expression levels of MUC2 and tight junction-related proteins, potentially influencing LPS translocation in the gut and the expression of serum inflammatory factors. Subsequent research revealed that the disparities in serum inflammatory cytokine levels between the HFD and the HFD + PS-MS groups were diminished following ABX treatment. This reduction is likely due to decreased translocation of LPSs from the gut into the bloodstream after the antibiotic treatment. Consequently, after neutralizing the differences in the

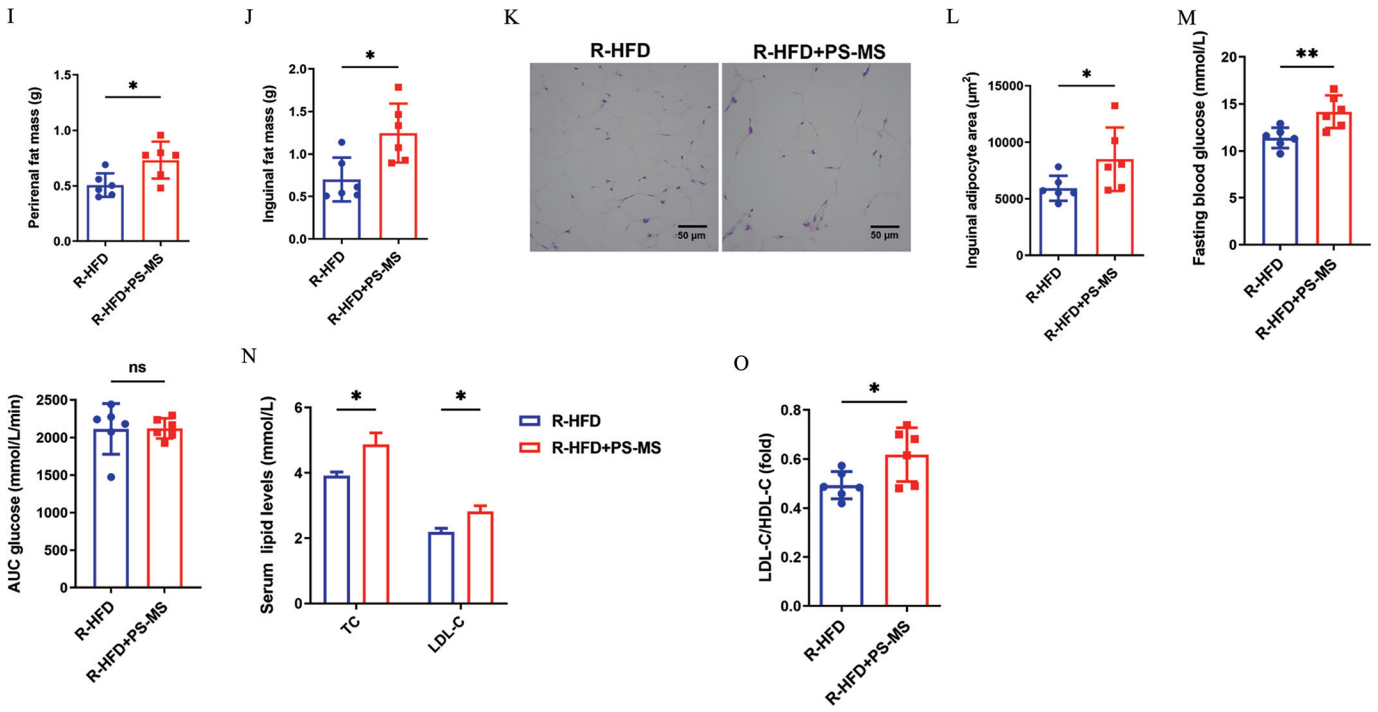

Figure 6. (*Continued.*)

expression levels of MUC2, tight junction-related proteins, and serum inflammation levels with the ABX, no significant differences in obesity-related outcomes—such as weight gain, liver weight, adipose tissue mass, and blood lipid levels—were observed. However, it is noteworthy that despite the ABX treatment, the lipid accumulation induced by the HFD was not entirely abrogated when compared with the ND diet, indicating that gut microbes participate in HFD-induced obesity but are not the sole determining factor.

Although the findings demonstrate that PS-MS contributed to HFD-induced obesity by altering the structure and composition of the gut microbiota, it remains to be further determined if the obesity phenotype in mice exposed to PS-MS depended on the modulating effects of the gut microbiota. In recent years, FMT has emerged as a promising method for establishing a cause-and-effect relationship between gut microbiota and obesity.[97] FMT involves transferring intestinal bacteria from donor mice to recipient mice through oral gavage. Therefore, FMT was employed in this study to examine the role of PS-MS–associated gut microbiota in exacerbating HFD-induced obesity. The experiment revealed no significant difference in food intake between the R-HFD + PS-MS treatment group and the R-HFD treatment group. However, the R-HFD + PS-MS treatment group exhibited greater hepatic lipid deposition and adipocyte size, suggesting that the pro-obesity effect of PS-MS might be partially mediated by intestinal bacteria. Furthermore, 16S rRNA sequencing results demonstrated that the microbial composition of the R-HFD group was similar to that of the HFD group, whereas the microbial composition of the R-HFD + PS-MS group differed from that of the HFD group but resembled that of the HFD + PS-MS group. These findings indicate successful colonization of recipient mice with the donor microbiota, partially reproducing the obesity-related phenotype. However, significant differences were observed only in fasting blood glucose levels, not in blood glucose AUC, potentially due to disruptions in the initial microbiome conditions, such as routine and sterile conditions. Transplanting the gut microbiota to germ-free mice would provide more compelling evidence to support these findings. At the same time, R-HFD + PS-MS mice demonstrated lower expression of MUC2 and *Tjp1*, and higher serum inflammation levels. Consequently, the dysbiosis of gut microbiota and lower expression of mRNA/proteins associated with intestinal integrity may have synergistically contributed to the progression of low-grade inflammation, a well-documented factor in promoting the development of obesity.[98] In addition, FMT from PS-MS + HFD-fed mice exacerbated HFD-induced obesity compared with FMT from HFD-fed mice into HFD-fed recipient mice, further supporting our conclusion that PS-MS induced a lower level of MUC2 protein expression, low-grade inflammation and obesity depended on intestinal flora.

Obesity and its associated chronic inflammatory diseases have emerged as significant health concerns, affecting both developed and developing countries alike.[99] Recent studies indicate that the relationship between obesity, gut barrier, intestinal microbes, and their interactions is interlinked and chiefly dependent on dietary habits.[100] Our study suggested that commercial PS-MS exacerbated HFD-driven changes of intestinal integrity, inflammation, and obesity by altering the gut microbiome. We observed that mice exposed to PS-MS demonstrated amplified HFD-induced microbiota dysbiosis, demonstrating a superimposed effect between PS-MS and HFD on intestinal integrity and flora. This highlights the importance of considering the impact of intestinal health on individuals with different dietary habits, particularly those consuming Western diets, given that PS-MS may enhance the progression of obesity via alterations in the microflora.

Conclusions

In summary, our study demonstrated that mice exposed to PS-MS of 5 μm in size had lower expression of mucus layer proteins (which may result in more toxic molecules entry into the body), higher expression of inflammatory cytokines, and exacerbation of HFD-induced obesity. Through antibiotic treatment and FMT

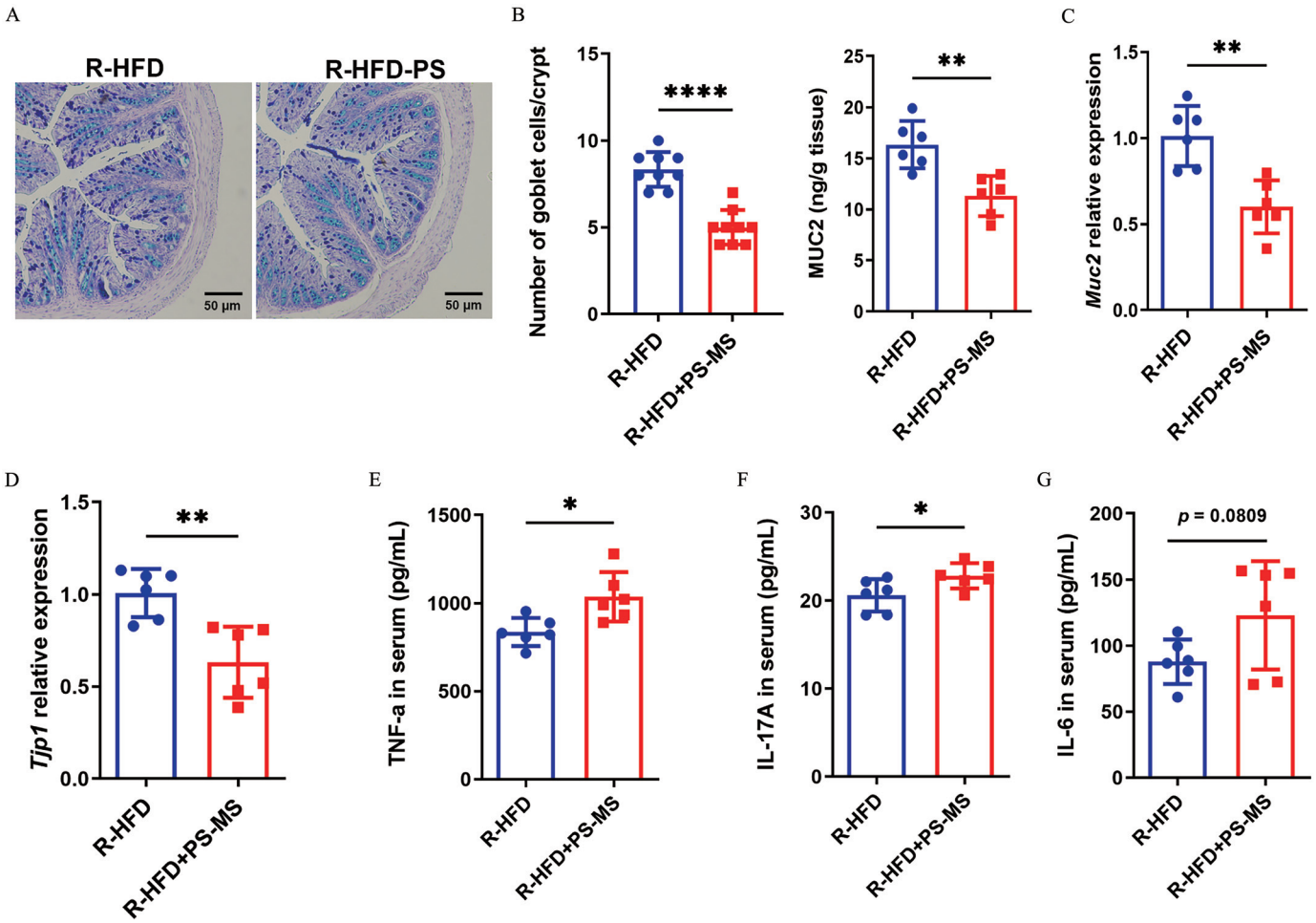

Figure 7. Effects of gut microbiota from HFD + PS-MS donor group on Muc2 and Tjp1 expression and inflammatory cytokines expression in microbiota-depleted, R-HFD mice for 8 wk. (A) Alcian blue/periodic acid-Schiff (AB/PAS) staining and quantification of goblet cell numbers from sections of distal colon stained with AB/PAS. Each data represents 1 crypt, 3 slices/group, 3 crypts/slice ($n = 9$). (B) MUC2 protein contents. (C) *Muc2* relative expression levels in colon tissue. (D) *Tjp1* relative expression levels in colon tissue. The level of (E) TNF-α, (F) IL-17A, (G) IL-6 in serum. Unless otherwise specified, data were analyzed using Student's *t*-test for comparisons between two groups. Data are represented as mean ± SD in scatter plots ($n = 6$ unless otherwise noted). Corresponding numeric data can be found in Table S3. Note: HFD, high-fat diet; IL, interleukin; PS-MS, polystyrene microspheres; R-HFD, HFD receivers; R-HFD + PS-MS, HFD + PS-MS receivers; SD, standard deviation; TNF, tumor necrosis factor. $^{*}p < 0.05$, $^{**}p < 0.01$ $^{****}p < 0.0001$.

experiments, we demonstrated that the microbiota play a critical role in the obesity process related to PS-MS exposure. Together, our results suggest that PS-MS promote HFD-induced obesity by altering gut microbiota. Although many other types of MPs exist widely in daily life, their effects on mucus–bacterial interactions remain largely unknown. Nevertheless, considering the inevitable human exposure to MPs and their potential toxicity link with obesity, it is important to monitor our exposure to these pollutants and their role in promoting inflammation, which may in turn lead to chronic metabolic diseases.

Acknowledgments

This work was supported by the National Key R&D Program of China (2022YFF1100102, 2022YFF1100104), the National Natural Science Foundation of China (No. 31625025), and the 2115 Talent Development Program of China Agricultural University.

The entirety of the data generated throughout this study has been comprehensively documented and is available within the main body of this article, as well as its supplementary information. The 16S rRNA raw reads are available at the National Center for Biotechnology Information (NCBI) Sequence Read Archive (SRA) repository (BioProject PRJNA990701).

References

1. Evers-van Gogh IJA, Oteng AB, Alex S, Hamers N, Catoire M, Stienstra R, et al. 2016. Muscle-specific inflammation induced by MCP-1 overexpression does not affect whole-body insulin sensitivity in mice. Diabetologia 59(3):624–633, PMID: 26661101, https://doi.org/10.1007/s00125-015-3822-2.
2. WHO (World Health Organization). 2024. Obesity and Overweight. https://www.who.int/news-room/fact-sheets/detail/obesity-and-overweight#:~:text=Worldwide%20obesity%20has%20nearly%20tripled,%2C%20and%2013%25%20were%20obese [accessed 12 August 2022].
3. Saltiel AR, Olefsky JM. 2017. Inflammatory mechanisms linking obesity and metabolic disease. J Clin Invest 127(1):1–4, PMID: 28045402, https://doi.org/10.1172/JCI92035.
4. Fabbrini E, Sullivan S, Klein S. 2010. Obesity and nonalcoholic fatty liver disease: biochemical, metabolic, and clinical implications. Hepatology 51(2):679–689, PMID: 20041406, https://doi.org/10.1002/hep.23280.
5. Ling C, Rönn T. 2019. Epigenetics in human obesity and type 2 diabetes. Cell Metab 29(5):1028–1044, PMID: 30982733, https://doi.org/10.1016/j.cmet.2019.03.009.
6. Hill JO, Melanson EL, Wyatt HT. 2000. Dietary fat intake and regulation of energy balance: implications for obesity. J Nutr 130(suppl 2S):284S–288S, PMID: 10721889, https://doi.org/10.1093/jn/130.2.284S.
7. Yin J, Li Y, Han H, Chen S, Gao J, Liu G, et al. 2018. Melatonin reprogramming of gut microbiota improves lipid dysmetabolism in high-fat diet-fed mice. J Pineal Res 65(4):e12524, PMID: 30230594, https://doi.org/10.1111/jpi.12524.
8. Ley RE, Bäckhed F, Turnbaugh P, Lozupone CA, Knight RD, Gordon JI. 2005. Obesity alters gut microbial ecology. Proc Natl Acad Sci USA 102(31):11070–11075, PMID: 16033867, https://doi.org/10.1073/pnas.0504978102.

9. Turnbaugh PJ, Ley RE, Mahowald MA, Magrini V, Mardis ER, Gordon JI. 2006. An obesity-associated gut microbiome with increased capacity for energy harvest. Nature 444(7122):1027–1031, PMID: 17183312, https://doi.org/10.1038/nature05414.
10. Chassaing B, Koren O, Goodrich JK, Poole AC, Srinivasan S, Ley RE, et al. 2015. Dietary emulsifiers impact the mouse gut microbiota promoting colitis and metabolic syndrome. Nature 519(7541):92–96, PMID: 25731162, https://doi.org/10.1038/nature14232.
11. Barnes DKA, Galgani F, Thompson RC, Barlaz M. 2009. Accumulation and fragmentation of plastic debris in global environments. Philos Trans R Soc Lond B Biol Sci 364(1526):1985–1998, PMID: 19528051, https://doi.org/10.1098/rstb.2008.0205.
12. Geyer R, Jambeck JR, Law KL. 2017. Production, use, and fate of all plastics ever made. Sci Adv 3(7):e1700782, PMID: 28776036, https://doi.org/10.1126/sciadv.1700782.
13. Zhao S, Zhu L, Li D. 2015. Microplastic in three urban estuaries, China. Environ Pollut 206:597–604, PMID: 26312741, https://doi.org/10.1016/j.envpol.2015.08.027.
14. Rochman CM, Browne MA, Halpern BS, Hentschel BT, Hoh E, Karapanagioti HK, et al. 2013. Policy: classify plastic waste as hazardous. Nature 494(7436):169–171, PMID: 23407523, https://doi.org/10.1038/494169a.
15. Vethaak AD, Legler J. 2021. Microplastics and human health. Science 371(6530):672–674, PMID: 33574197, https://doi.org/10.1126/science.abe5041.
16. Wu P, Lin S, Cao G, Wu J, Jin H, Wang C, et al. 2022. Absorption, distribution, metabolism, excretion and toxicity of microplastics in the human body and health implications. J Hazard Mater 437:129361, PMID: 35749897, https://doi.org/10.1016/j.jhazmat.2022.129361.
17. Zuccarello P, Ferrante M, Cristaldi A, Copat C, Grasso A, Sangregorio D, et al. 2019. Exposure to microplastics (<10 μm) associated to plastic bottles mineral water consumption: the first quantitative study. Water Res 157:365–371, PMID: 30974285, https://doi.org/10.1016/j.watres.2019.03.091.
18. Lee M-R, Lai F-Y, Dou J, Lin K-L, Chung L-W. 2011. Determination of trace leaching phthalate esters in water and urine from plastic containers by solid-phase microextraction and gas chromatography-mass spectrometry. Anal Lett 44(4):676–686, https://doi.org/10.1080/00032711003783077.
19. Zhang J, Wang L, Trasande L, Kannan K. 2021. Occurrence of polyethylene terephthalate and polycarbonate microplastics in infant and adult feces. Environ Sci Technol Lett 8(11):989–994, https://doi.org/10.1021/acs.estlett.1c00559.
20. Leslie HA, van Velzen MJM, Brandsma SH, Vethaak AD, Garcia-Vallejo JJ, Lamoree MH. 2022. Discovery and quantification of plastic particle pollution in human blood. Environ Int 163:107199, PMID: 35367073, https://doi.org/10.1016/j.envint.2022.107199.
21. Ibrahim YS, Tuan Anuar S, Azmi AA, Wan Mohd Khalik WMA, Lehata S, Hamzah SR, et al. 2020. Detection of microplastics in human colectomy specimens. JGH Open 5(1):116–121, PMID: 33490620, https://doi.org/10.1002/jgh3.12457.
22. Braun T, Ehrlich L, Henrich W, Koeppel S, Lomako I, Schwabl P, et al. 2021. Detection of microplastic in human placenta and meconium in a clinical setting. Pharmaceutics 13(7):921, PMID: 34206212, https://doi.org/10.3390/pharmaceutics13070921.
23. Schymanski D, Goldbeck C, Humpf HU, Fürst P. 2018. Analysis of microplastics in water by micro-Raman spectroscopy: release of plastic particles from different packaging into mineral water. Water Res 129:154–162, PMID: 29145085, https://doi.org/10.1016/j.watres.2017.11.011.
24. Kik K, Bukowska B, Sicińska P. 2020. Polystyrene nanoparticles: sources, occurrence in the environment, distribution in tissues, accumulation and toxicity to various organisms. Environ Pollut 262:114297, PMID: 32155552, https://doi.org/10.1016/j.envpol.2020.114297.
25. Deng Y, Zhang Y, Lemos B, Ren H. 2017. Tissue accumulation of microplastics in mice and biomarker responses suggest widespread health risks of exposure. Sci Rep 7:46687, PMID: 28436478, https://doi.org/10.1038/srep46687.
26. Jin Y, Lu L, Tu W, Luo T, Fu Z. 2019. Impacts of polystyrene microplastic on the gut barrier, microbiota and metabolism of mice. Sci Total Environ 649:308–317, PMID: 30176444, https://doi.org/10.1016/j.scitotenv.2018.08.353.
27. Jing J, Zhang L, Han L, Wang J, Zhang W, Liu Z, et al. 2022. Polystyrene micro-/nanoplastics induced hematopoietic damages via the crosstalk of gut microbiota, metabolites, and cytokines. Environ Int 161:107131, PMID: 35149446, https://doi.org/10.1016/j.envint.2022.107131.
28. Qiao R, Sheng C, Lu Y, Zhang Y, Ren H, Lemos B. 2019. Microplastics induce intestinal inflammation, oxidative stress, and disorders of metabolome and microbiome in zebrafish. Sci Total Environ 662:246–253, PMID: 30690359, https://doi.org/10.1016/j.scitotenv.2019.01.245.
29. Lu Y, Zhang Y, Deng Y, Jiang W, Zhao Y, Geng J, et al. 2016. Uptake and accumulation of polystyrene microplastics in zebrafish (*Danio rerio*) and toxic effects in liver. Environ Sci Technol 50(7):4054–4060, PMID: 26950772, https://doi.org/10.1021/acs.est.6b00183.
30. Jin H, Ma T, Sha X, Liu Z, Zhou Y, Meng X, et al. 2021. Polystyrene microplastics induced male reproductive toxicity in mice. J Hazard Mater 401:123430, PMID: 32659591, https://doi.org/10.1016/j.jhazmat.2020.123430.
31. Li B, Ding Y, Cheng X, Sheng D, Xu Z, Rong Q, et al. 2020. Polyethylene microplastics affect the distribution of gut microbiota and inflammation development in mice. Chemosphere 244:125492, PMID: 31809927, https://doi.org/10.1016/j.chemosphere.2019.125492.
32. Liang B, Zhong Y, Huang Y, Lin X, Liu J, Lin L, et al. 2021. Underestimated health risks: polystyrene micro- and nanoplastics jointly induce intestinal barrier dysfunction by ROS-mediated epithelial cell apoptosis. Part Fibre Toxicol 18(1):20, PMID: 34098985, https://doi.org/10.1186/s12989-021-00414-1.
33. Yang J-Z, Zhang K-K, Liu Y, Li X-W, Chen L-J, Liu J-L, et al. 2023. Epigallocatechin-3-gallate ameliorates polystyrene microplastics-induced anxiety-like behavior in mice by modulating gut microbe homeostasis. Sci Total Environ 892:164619, PMID: 37269995, https://doi.org/10.1016/j.scitotenv.2023.164619.
34. Zhang K, Yang J, Chen L, He J, Qu D, Zhang Z, et al. 2023. Gut microbiota participates in polystyrene microplastics-induced hepatic injuries by modulating the gut–liver axis. ACS Nano 17(15):15125–15145, PMID: 37486121, https://doi.org/10.1021/acsnano.3c04449.
35. Ridaura VK, Faith JJ, Rey FE, Cheng J, Duncan AE, Kau AL, et al. 2013. Gut microbiota from twins discordant for obesity modulate metabolism in mice. Science 341(6150):1241214, PMID: 24009397, https://doi.org/10.1126/science.1241214.
36. Cani PD, Possemiers S, Van de Wiele T, Guiot Y, Everard A, Rottier O, et al. 2009. Changes in gut microbiota control inflammation in obese mice through a mechanism involving GLP-2-driven improvement of gut permeability. Gut 58(8):1091–1103, PMID: 19240062, https://doi.org/10.1136/gut.2008.165886.
37. Hu C, Liu M, Tang L, Liu H, Sun B, Chen L. 2021. Probiotic intervention mitigates the metabolic disturbances of perfluorobutanesulfonate along the gut-liver axis of zebrafish. Chemosphere 284:131374, PMID: 34217933, https://doi.org/10.1016/j.chemosphere.2021.131374.
38. Zheng H, Wang J, Wei X, Chang L, Liu S. 2021. Proinflammatory properties and lipid disturbance of polystyrene microplastics in the livers of mice with acute colitis. Sci Total Environ 750:143085, PMID: 33182181, https://doi.org/10.1016/j.scitotenv.2020.143085.
39. Kleiner DE, Brunt EM, Van Natta M, Behling C, Contos MJ, Cummings OW, et al. 2005. Design and validation of a histological scoring system for nonalcoholic fatty liver disease. Hepatology 41(6):1313–1321, PMID: 15915461, https://doi.org/10.1002/hep.20701.
40. Schneider CA, Rasband WS, Eliceiri KW. 2012. NIH image to ImageJ: 25 years of image analysis. Nat Methods 9(7):671–675, PMID: 22930834, https://doi.org/10.1038/nmeth.2089.
41. da Costa RM, Neves KB, Mestriner FL, Louzada-Junior P, Bruder-Nascimento T, Tostes RC. 2016. TNF-α induces vascular insulin resistance via positive modulation of PTEN and decreased akt/eNOS/NO signaling in high fat diet-fed mice. Cardiovasc Diabetol 15(1):119, PMID: 27562094, https://doi.org/10.1186/s12933-016-0443-0.
42. Caporaso JG, Kuczynski J, Stombaugh J, Bittinger K, Bushman FD, Costello EK, et al. 2010. QIIME allows analysis of high-throughput community sequencing data. Nat Methods 7(5):335–336, PMID: 20383131, https://doi.org/10.1038/nmeth.f.303.
43. Zarrinpar A, Chaix A, Xu ZZ, Chang MW, Marotz CA, Saghatelian A, et al. 2018. Antibiotic-induced microbiome depletion alters metabolic homeostasis by affecting gut signaling and colonic metabolism. Nat Commun 9(1):2872, PMID: 30030441, https://doi.org/10.1038/s41467-018-05336-9.
44. Zhao Q, Yu J, Zhou H, Wang X, Zhang C, Hu J, et al. 2023. Intestinal dysbiosis exacerbates the pathogenesis of psoriasis-like phenotype through changes in fatty acid metabolism. Signal Transduct Target Ther 8(1):40, PMID: 36710269, https://doi.org/10.1038/s41392-022-01219-0.
45. Zhang B, Fan X, Du H, Zhao M, Zhang Z, Zhu R, et al. 2023. Foodborne carbon dot exposure induces insulin resistance through gut microbiota dysbiosis and damaged intestinal mucus layer. ACS Nano 17(6):6081–6094, PMID: 36897192, https://doi.org/10.1021/acsnano.3c01005.
46. Borody TJ, Paramsothy S, Agrawal G. 2013. Fecal microbiota transplantation: indications, methods, evidence, and future directions. Curr Gastroenterol Rep 15(8):337, PMID: 23852569, https://doi.org/10.1007/s11894-013-0337-1.
47. Brun P, Castagliuolo I, Di Leo V, Buda A, Pinzani M, Palù G, et al. 2007. Increased intestinal permeability in obese mice: new evidence in the pathogenesis of nonalcoholic steatohepatitis. Am J Physiol Gastrointest Liver Physiol 292(2):G518–G525, PMID: 17023554, https://doi.org/10.1152/ajpgi.00024.2006.
48. Yoseph BP, Klingensmith NJ, Liang Z, Breed ER, Burd EM, Mittal R, et al. 2016. Mechanisms of intestinal barrier dysfunction in sepsis. Shock 46(1):52–59, PMID: 27299587, https://doi.org/10.1097/SHK.0000000000000565.
49. Benjamin JL, Sumpter R Jr, Levine B, Hooper LV. 2013. Intestinal epithelial autophagy is essential for host defense against invasive bacteria. Cell Host Microbe 13(6):723–734, PMID: 23768496, https://doi.org/10.1016/j.chom.2013.05.004.

50. Yu J, Chen X, Zhang Y, Cui X, Zhang Z, Guo W, et al. 2022. Antibiotic azithromycin inhibits brown/beige fat functionality and promotes obesity in human and rodents. Theranostics 12(3):1187–1203, PMID: 35154482, https://doi.org/10.7150/thno.63067.
51. Xu D, Ma Y, Han X, Chen Y. 2021. Systematic toxicity evaluation of polystyrene nanoplastics on mice and molecular mechanism investigation about their internalization into Caco-2 cells. J Hazard Mater 417:126092, PMID: 34015712, https://doi.org/10.1016/j.jhazmat.2021.126092.
52. Liu S, Li H, Wang J, Wu B, Guo X. 2022. Polystyrene microplastics aggravate inflammatory damage in mice with intestinal immune imbalance. Sci Total Environ 833:155198, PMID: 35427627, https://doi.org/10.1016/j.scitotenv.2022.155198.
53. Senathirajah K, Attwood S, Bhagwat G, Carbery M, Wilson S, Palanisami T. 2021. Estimation of the mass of microplastics ingested—a pivotal first step towards human health risk assessment. J Hazard Mater 404(pt B):124004, PMID: 33130380, https://doi.org/10.1016/j.jhazmat.2020.124004.
54. Koelmans AA, Mohamed Nor NH, Hermsen E, Kooi M, Mintenig SM, De France J. 2019. Microplastics in freshwaters and drinking water: critical review and assessment of data quality. Water Res 155:410–422, PMID: 30861380, https://doi.org/10.1016/j.watres.2019.02.054.
55. Sangkham S, Faikhaw O, Munkong N, Sakunkoo P, Arunlertaree C, Chavali M, et al. 2022. A review on microplastics and nanoplastics in the environment: their occurrence, exposure routes, toxic studies, and potential effects on human health. Mar Pollut Bull 181:113832, PMID: 35716489, https://doi.org/10.1016/j.marpolbul.2022.113832.
56. Shiu HT, Pan X, Liu Q, Long K, Cheng KKY, Ko BC-B, et al. 2022. Dietary exposure to polystyrene nanoplastics impairs fasting-induced lipolysis in adipose tissue from high-fat diet fed mice. J Hazard Mater 440:129698, PMID: 35952428, https://doi.org/10.1016/j.jhazmat.2022.129698.
57. Chen J, Wang M, Zhang P, Li H, Qu K, Xu R, et al. 2022. Cordycepin alleviated metabolic inflammation in Western diet-fed mice by targeting intestinal barrier integrity and intestinal flora. Pharmacol Res 178:106191, PMID: 35346845, https://doi.org/10.1016/j.phrs.2022.106191.
58. Huang T, Song J, Gao J, Cheng J, Xie H, Zhang L, et al. 2022. Adipocyte-derived kynurenine promotes obesity and insulin resistance by activating the AhR/STAT3/IL-6 signaling. Nat Commun 13(1):3489, PMID: 35715443, https://doi.org/10.1038/s41467-022-31126-5.
59. Huang H, Wei F, Qiu S, Xing B, Hou J. 2023. Polystyrene microplastics trigger adiposity in mice by remodeling gut microbiota and boosting fatty acid synthesis. Sci Total Environ 890:164297, PMID: 37211133, https://doi.org/10.1016/j.scitotenv.2023.164297.
60. Okamura T, Hamaguchi M, Hasegawa Y, Hashimoto Y, Majima S, Senmaru T, et al. 2023. Oral exposure to polystyrene microplastics of mice on a normal or high-fat diet and intestinal and metabolic outcomes. Environ Health Perspect 131(2):027006, PMID: 36821708, https://doi.org/10.1289/EHP11072.
61. Suárez-Zamorano N, Fabbiano S, Chevalier C, Stojanović O, Colin DJ, Stevanović A, et al. 2015. Microbiota depletion promotes browning of white adipose tissue and reduces obesity. Nat Med 21(12):1497–1501, PMID: 26569380, https://doi.org/10.1038/nm.3994.
62. Hildebrandt MA, Hoffmann C, Sherrill-Mix SA, Keilbaugh SA, Hamady M, Chen Y-Y, et al. 2009. High-fat diet determines the composition of the murine gut microbiome independently of obesity. Gastroenterology 137(5):1716–1724.e2, PMID: 19706296, https://doi.org/10.1053/j.gastro.2009.08.042.
63. Turnbaugh PJ, Bäckhed F, Fulton L, Gordon JI. 2008. Diet-induced obesity is linked to marked but reversible alterations in the mouse distal gut microbiome. Cell Host Microbe 3(4):213–223, PMID: 18407065, https://doi.org/10.1016/j.chom.2008.02.015.
64. Rizzatti G, Lopetuso LR, Gibiino G, Binda C, Gasbarrini A. 2017. Proteobacteria: a common factor in human diseases. Biomed Res Int 2017:9351507, PMID: 29230419, https://doi.org/10.1155/2017/9351507.
65. Cho I, Yamanishi S, Cox L, Methé BA, Zavadil J, Li K, et al. 2012. Antibiotics in early life alter the murine colonic microbiome and adiposity. Nature 488(7413):621–626, PMID: 22914093, https://doi.org/10.1038/nature11400.
66. Tun HM, Bridgman SL, Chari R, Field CJ, Guttman DS, Becker AB, et al. 2018. Roles of birth mode and infant gut microbiota in intergenerational transmission of overweight and obesity from mother to offspring. JAMA Pediatr 172(4):368–377, PMID: 29459942, https://doi.org/10.1001/jamapediatrics.2017.5535.
67. Takeuchi T, Kameyama K, Miyauchi E, Nakanishi Y, Kanaya T, Fujii T, et al. 2023. Fatty acid overproduction by gut commensal microbiota exacerbates obesity. Cell Metab 35(2):361–375.e9, PMID: 36652945, https://doi.org/10.1016/j.cmet.2022.12.013.
68. Mo S-J, Lee K, Hong H-J, Hong D-K, Jung S-H, Park S-D, et al. 2022. Effects of *Lactobacillus curvatus* HY7601 and *Lactobacillus plantarum* KY1032 on overweight and the gut microbiota in humans: randomized, double-blinded, placebo-controlled clinical trial. Nutrients 14(12):2484, PMID: 35745214, https://doi.org/10.3390/nu14122484.
69. Cani PD, Bibiloni R, Knauf C, Waget A, Neyrinck AM, Delzenne NM, et al. 2008. Changes in gut microbiota control metabolic endotoxemia-induced inflammation in high-fat diet–induced obesity and diabetes in mice. Diabetes 57(6):1470–1481, PMID: 18305141, https://doi.org/10.2337/db07-1403.
70. Pan X, Kaminga AC, Liu A, Wen SW, Luo M, Luo J. 2021. Gut microbiota, glucose, lipid, and water-electrolyte metabolism in children with nonalcoholic fatty liver disease. Front Cell Infect Microbiol 11:683743, PMID: 34778099, https://doi.org/10.3389/fcimb.2021.683743.
71. Anhê FF, Marette A. 2017. A microbial protein that alleviates metabolic syndrome. Nat Med 23(1):11–12, PMID: 28060804, https://doi.org/10.1038/nm.4261.
72. Cirstea M, Radisavljevic N, Finlay BB. 2018. Good bug, bad bug: breaking through microbial stereotypes. Cell Host Microbe 23(1):10–13, PMID: 29324224, https://doi.org/10.1016/j.chom.2017.12.008.
73. Tokuhara D, Kurashima Y, Kamioka M, Nakayama T, Ernst P, Kiyono H. 2019. A comprehensive understanding of the gut mucosal immune system in allergic inflammation. Allergol Int 68(1):17–25, PMID: 30366757, https://doi.org/10.1016/j.alit.2018.09.004.
74. Everard A, Belzer C, Geurts L, Ouwerkerk JP, Druart C, Bindels LB, et al. 2013. Cross-talk between *Akkermansia muciniphila* and intestinal epithelium controls diet-induced obesity. Proc Natl Acad Sci USA 110(22):9066–9071, PMID: 23671105, https://doi.org/10.1073/pnas.1219451110.
75. Plovier H, Everard A, Druart C, Depommier C, Van Hul M, Geurts L, et al. 2017. A purified membrane protein from *Akkermansia muciniphila* or the pasteurized bacterium improves metabolism in obese and diabetic mice. Nat Med 23(1):107–113, PMID: 27892954, https://doi.org/10.1038/nm.4236.
76. Zheng H, Liang H, Wang Y, Miao M, Shi T, Yang F, et al. 2016. Altered gut microbiota composition associated with eczema in infants. PLoS One 11(11):e0166026, PMID: 27812181, https://doi.org/10.1371/journal.pone.0166026.
77. Khan S, Waliullah S, Godfrey V, Khan MAW, Ramachandran RA, Cantarel BL, et al. 2020. Dietary simple sugars alter microbial ecology in the gut and promote colitis in mice. Sci Transl Med 12(567):eaay6218, PMID: 33115951, https://doi.org/10.1126/scitranslmed.aay6218.
78. Daniel H, Gholami AM, Berry D, Desmarchelier C, Hahne H, Loh G, et al. 2014. High-fat diet alters gut microbiota physiology in mice. ISME J 8(2):295–308, PMID: 24030595, https://doi.org/10.1038/ismej.2013.155.
79. Dai Z, Feng S, Liu AB, Wang H, Zeng X, Yang CS. 2019. Protective effects of α-galacto-oligosaccharides against a high-fat/western-style diet-induced metabolic abnormalities in mice. Food Funct 10(6):3660–3670, PMID: 31166330, https://doi.org/10.1039/c9fo00463g.
80. Wang J, Tang H, Zhang C, Zhao Y, Derrien M, Rocher E, et al. 2015. Modulation of gut microbiota during probiotic-mediated attenuation of metabolic syndrome in high fat diet-fed mice. ISME J 9(1):1–15, PMID: 24936764, https://doi.org/10.1038/ismej.2014.99.
81. Chang T-T, Chen J-W. 2021. Direct CCL4 inhibition modulates gut microbiota, reduces circulating trimethylamine N-oxide, and improves glucose and lipid metabolism in high-fat-diet-induced diabetes mellitus. J Inflamm Res 14:6237–6250, PMID: 34866923, https://doi.org/10.2147/JIR.S343491.
82. Parnell JA, Reimer RA. 2012. Prebiotic fiber modulation of the gut microbiota improves risk factors for obesity and the metabolic syndrome. Gut Microbes 3(1):29–34, PMID: 22555633, https://doi.org/10.4161/gmic.19246.
83. Cani PD, Amar J, Iglesias MA, Poggi M, Knauf C, Bastelica D, et al. 2007. Metabolic endotoxemia initiates obesity and insulin resistance. Diabetes 56(7):1761–1772, PMID: 17456850, https://doi.org/10.2337/db06-1491.
84. Cani PD, Neyrinck AM, Fava F, Knauf C, Burcelin RG, Tuohy KM, et al. 2007. Selective increases of bifidobacteria in gut microflora improve high-fat-diet-induced diabetes in mice through a mechanism associated with endotoxaemia. Diabetologia 50(11):2374–2383, PMID: 17823788, https://doi.org/10.1007/s00125-007-0791-0.
85. Wu T-R, Lin C-S, Chang C-J, Lin T-L, Martel J, Ko Y-F, et al. 2019. Gut commensal *Parabacteroides goldsteinii* plays a predominant role in the anti-obesity effects of polysaccharides isolated from *Hirsutella sinensis*. Gut 68(2):248–262, PMID: 30007918, https://doi.org/10.1136/gutjnl-2017-315458.
86. Turner JR. 2009. Intestinal mucosal barrier function in health and disease. Nat Rev Immunol 9(11):799–809, PMID: 19855405, https://doi.org/10.1038/nri2653.
87. Schroeder BO, Birchenough GMH, Ståhlman M, Arike L, Johansson MEV, Hansson GC, et al. 2018. Bifidobacteria or fiber protects against diet-induced microbiota-mediated colonic mucus deterioration. Cell Host Microbe 23(1):27–40.e7, PMID: 29276171, https://doi.org/10.1016/j.chom.2017.11.004.
88. Dunleavy KA, Raffals LE, Camilleri M. 2023. Intestinal barrier dysfunction in inflammatory bowel disease: underpinning pathogenesis and therapeutics. Dig Dis Sci 68(12):4306–4320, PMID: 37773554, https://doi.org/10.1007/s10620-023-08122-w.
89. Fan X, Yao H, Liu X, Shi Q, Lv L, Li P, et al. 2020. High-fat diet alters the expression of reference genes in male mice. Front Nutr 7:589771, PMID: 33330591, https://doi.org/10.3389/fnut.2020.589771.
90. Forlano R, Mullish BH, Roberts LA, Thursz MR, Manousou P. 2022. The intestinal barrier and its dysfunction in patients with metabolic diseases and non-alcoholic fatty liver disease. Int J Mol Sci 23(2):662, PMID: 35054847, https://doi.org/10.3390/ijms23020662.

91. Donaldson GP, Lee SM, Mazmanian SK. 2016. Gut biogeography of the bacterial microbiota. Nat Rev Microbiol 14(1):20–32, PMID: 26499895, https://doi.org/10.1038/nrmicro3552.
92. Karst SM. 2016. The influence of commensal bacteria on infection with enteric viruses. Nat Rev Microbiol 14(4):197–204, PMID: 26853118, https://doi.org/10.1038/nrmicro.2015.25.
93. Li K, Zhang L, Xue J, Yang X, Dong X, Sha L, et al. 2019. Dietary inulin alleviates diverse stages of type 2 diabetes mellitus via anti-inflammation and modulating gut microbiota in db/db mice. Food Funct 10(4):1915–1927, PMID: 30869673, https://doi.org/10.1039/c8fo02265h.
94. Huang D, Zhang Y, Long J, Yang X, Bao L, Yang Z, et al. 2022. Polystyrene microplastic exposure induces insulin resistance in mice via dysbacteriosis and pro-inflammation. Sci Total Environ 838(pt 1):155937, PMID: 35588841, https://doi.org/10.1016/j.scitotenv.2022.155937.
95. Cox LM, Yamanishi S, Sohn J, Alekseyenko AV, Leung JM, Cho I, et al. 2014. Altering the intestinal microbiota during a critical developmental window has lasting metabolic consequences. Cell 158(4):705–721, PMID: 25126780, https://doi.org/10.1016/j.cell.2014.05.052.
96. Xiao S, Fei N, Pang X, Shen J, Wang L, Zhang B, et al. 2014. A gut microbiota-targeted dietary intervention for amelioration of chronic inflammation underlying metabolic syndrome. FEMS Microbiol Ecol 87(2):357–367, PMID: 24117923, https://doi.org/10.1111/1574-6941.12228.
97. Lu X, Liu J, Zhang N, Fu Y, Zhang Z, Li Y, et al. 2019. Ripened Pu-erh tea extract protects mice from obesity by modulating gut microbiota composition. J Agric Food Chem 67(25):6978–6994, PMID: 31070363, https://doi.org/10.1021/acs.jafc.8b04909.
98. Gentile CL, Weir TL. 2018. The gut microbiota at the intersection of diet and human health. Science 362(6416):776–780, PMID: 30442802, https://doi.org/10.1126/science.aau5812.
99. Gregor MF, Hotamisligil GS. 2011. Inflammatory mechanisms in obesity. Annu Rev Immunol 29:415–445, PMID: 21219177, https://doi.org/10.1146/annurev-immunol-031210-101322.
100. GBD 2015 Obesity Collaborators, Afshin AMH, Forouzanfar MB, Reitsma P, Sur K, Estep A, et al. 2017. Health effects of overweight and obesity in 195 countries over 25 years. N Engl J Med 377(1):13–27, PMID: 28604169, https://doi.org/10.1056/NEJMoa1614362.